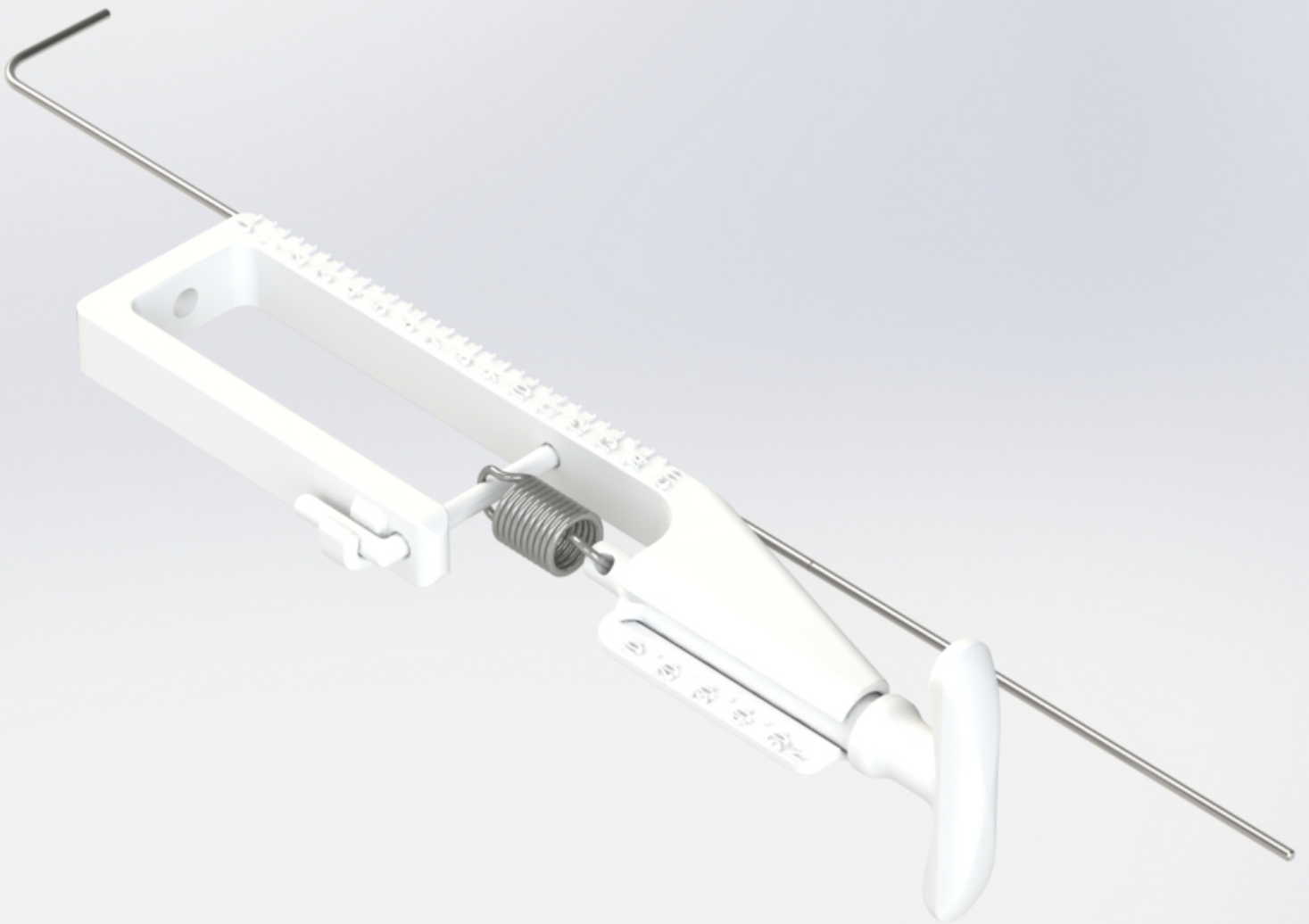


MINT

Minimally invasive tensiometry:
a device to quantify tension during laparoscopic
herniorrhaphy

Master thesis
M.F. Wempe



Preface

Dear reader,

Six years ago, I began my bachelor's in Mechanical Engineering at TU Delft. After four years of mathematics, physics, and a bit of designing, I realized that technical design was more for me. Designs with requirements beyond the mechanical field captured my attention, particularly those involving users and their unique problems. My master's in BioMedical Engineering provided numerous opportunities to work on such problems, and this project is a prime example.

Last year, I started an internship at Reinier de Graaf hospital under the supervision of Dr. A.L.A. Bloemendaal. During this internship, I frequently observed surgeries in the operating room, witnessing fascinating procedures. It was during one of these surgeries that Dr. A.L.A. Bloemendaal first expressed his desire for a device which can provide intraoperative information during abdominal wall surgeries to enhance surgical outcomes. Initially, I was not interested and even recommended some friends for the project. However, when he mentioned the (to me, magical) number: 30, I was hooked. This number corresponds to the percentage of patients experiencing issues after an abdominal wall hernia repair. Given that abdominal wall hernia repairs are among the most frequently performed general surgeries, 30% represents a substantial number of patients. By designing such a device, I could potentially improve the quality of life for many patients worldwide.

Dr A.L.A. Bloemendaal proved to be an excellent mentor throughout this whole journey, allowing me to observe even more intriguing surgeries and providing explanations for everything I wanted and needed to know. His passion and dedication to his craft motivated me to strive for the best possible outcomes. Additionally, I would like to thank my TU Delft supervisor, Prof. Dr. J.J van den Dobbelsteen, for his guidance and for taking the time to discuss challenges with me. I also extend my gratitude to Ing. J. van Frankenhuyzen, who assisted me during the conceptualization phase and connected me to the manufacturer of the final design.

Finally, I would like to thank my parents, family, and friends for their everlasting support, motivation, and guidance. This journey would not have been the same without them.

I am excited to see what the future holds for MINT. I hope this design can be a step towards better ventral hernia repair and, eventually, improve the lives of many patients.

I wish you a pleasant reading,

*M.F. Wempe
Delft, August 2024*

Abstract

Herniorrhaphy, the closure of an abdominal wall hernia, is one of the most performed general surgeries worldwide. However, approximately one-third of these patients require revision surgery due to hernia recurrence, possibly caused by excess tension on the aponeurotic edge. Currently, there is no standardized method to quantify this tension. This thesis aims to design a device for use in minimally invasive herniorrhaphy to provide intraoperative information on fascial tension to assist surgeons in intraoperative decision-making.

This thesis builds upon the work of E.F. van Koten, who designed an initial device called MINT based on a linear force spring to assess tension. However, her design was not yet suitable for intraoperative use due to small components and a high component count. Therefore, this thesis focuses on redesigning the MINT to reduce the complexity of the device.

Through the redesign of the connection mechanism, the component count was reduced from fourteen (and one tool) to five. This reduction has several advantages: it simplifies the device assembly and disassembly and reduces the risk of losing components. Consequently, the new design is more suitable for use in the operating room.

Further studies should investigate the reusability of the device made from selective laser sintered PA-12, and clinical testing is required before clinical implementation.

Contents

Preface	iii
Abstract	v
Nomenclature	xiii
1 Introduction	1
1.1 Herniorrhaphy	1
1.2 Problem statement	1
1.3 Research objective	2
2 Background	3
2.1 Anatomy of the abdominal wall	3
2.2 Abdominal wall hernia	3
2.3 Ventral hernia repair techniques	4
2.4 Clinical importance	4
2.5 MINT by E.F. van Koten	5
3 Methods	7
3.1 Design process	7
3.2 Thesis structure	7
4 Problem Analysis	9
4.1 Components	9
4.1.1 Number of components	9
4.1.2 Size of the components	10
4.2 Research objective	10
4.3 Requirements	10
5 Literature Study	13
6 Conceptualization	15
6.1 Connection between laparoscopic grasper and MINT	15
6.1.1 Cylindrical coupler block	15
6.1.2 Integrated coupler piece in main body	16
6.1.3 Choice of connecting mechanism to the laparoscopic forceps	16
6.2 Mechanical force gauge	16
6.2.1 Spring	16
6.2.2 Connection between main body and the spring	17
6.2.3 Straight guide	17
6.3 Distance measurement	18
6.3.1 Concept solutions	18
6.3.2 Criteria	20
7 MINT - Final Design	21
7.1 Design	21
7.2 Materials and manufacturing	22
7.3 Procedure	23
7.4 Costs	23
7.4.1 One device	23
7.4.2 One hundred devices	24

8	Verification	25
8.1	Force measurement	25
8.2	Assembly and disassembly time	26
8.3	Steam sterilization	27
8.4	Finite element analysis	28
8.5	Verification summary	29
8.5.1	Sterilization	29
8.5.2	Width	29
8.5.3	Clinical validation	30
9	Discussion	31
9.1	Limitations	31
9.2	Recommendations	32
10	Conclusion	35
	References	37
	Appendices	39
A	Spring Calibration	41
B	Harris Profile Scores	43
C	General Dimensions MINT	45
D	Instruction Manual	49
E	Verification Data	55
E.1	Force measurement test	55
E.2	Assembly and disassembly test	57

List of Figures

2.1	Cross-sectional diagram showing the anatomy of the abdominal wall.	3
2.2	Protrusion of intestines in an abdominal wall hernia.	4
2.3	Mesh placement options.	5
2.4	Overview of the design by E.F. van Koten.	5
3.1	Flowchart displaying the design process.	7
4.1	Components of the original MINT grouped based on their function within the device.	9
4.2	Medical instrument tray.	10
4.3	Components of the original MINT that could fall through the mesh of an instrument tray.	10
5.1	Schematic representation of the connection principles of group A, B, C and D.	13
6.1	Three different connection mechanisms discussed in Section 6.1.	15
6.2	Two considered connection options to connect the spring to the main body.	17
6.3	Two possible force scale placements.	17
6.4	Schematic drawing of the displacement of the abdominal wall defect.	18
6.5	Six concept solutions for measuring the travelled distance.	19
7.1	Isometric drawings of the final design.	21
7.2	Components of the final design.	21
7.3	Handles present in the original MINT and the final design.	22
7.4	MINT mounted on a laparoscopic grasper.	23
8.1	Setup of the force verification.	25
8.2	Visual representation of the measured errors in the force verification measurements.	26
8.3	Visual representation of the measured assembly and disassembly times.	26
8.4	Deformation present in the main body after steam sterilization.	27
8.5	FEA plots of the L-shaped link.	28
8.6	Width of the final design.	30
A.1	Force deflection curves of the spring.	41
C.1	Technical drawing of the main body.	45
C.2	Technical drawing of the L-shaped link.	46
C.3	Technical drawing of the handle.	46
C.4	Technical drawing of the distance indicator.	47

List of Tables

4.1	Device requirements.	11
5.1	Harris profile assessing the five identified connecting mechanism groups.	14
6.1	Spring specifications provided by the manufacturer.	16
6.2	Harris profile assessing the six distance measurement concepts.	20
7.1	Production costs of one device.	24
7.2	Production costs per 100 devices.	24
8.1	Used sterilization program.	27
8.2	Verification of requirements.	29
A.1	Data of the spring calibration.	41
B.1	Reasoning behind the Harris profile in Subsection 6.2.	44
E.1	Force gauge verification data.	56
E.2	Assembly and disassembly verification data.	57

Nomenclature

Abbreviations

Abbreviation	Definition
DSMH	Deskundige Sterile Medische Hulpmiddelen (expert on sterile medical devices)
FEA	Finite Element Analysis
MINT	Minimally Invasive Tensiometry
MIS	Minimally Invasive Surgery
OR	Operating Room
PA-12	Polyamide 12
PP	Polypropylene
RdGG	Reinier de Graaf Gasthuis
SLS	Selective Laser Sintering (3D-printing technique)
SS	Stainless Steel

Symbols

Symbol	Definition	Unit
C	Spring constant	[N/mm]
F	Force	[N]
F_0	Pre-tension	[N]
L_0	Initial length	[mm]
S_n	Maximum spring force	[N]
δ	Deflection	[mm]
ρ	Density	[g/cm ³]

1

Introduction

Herniorrhaphy, the closure of an abdominal wall hernia, is one of the most performed general surgeries worldwide, with a notable increase in prevalence over the last thirty years. This rise could be attributed to factors such as the increasing number of intra-abdominal surgeries resulting in more incisional hernias, increasing obesity rates and a high recurrence rate [1, 2]. Revision surgery is required in nearly one-third of patients due to hernia recurrence [3]. This thesis aims to design a device to quantify abdominal wall tension minimally invasively to aid in surgical decision making.

1.1. Herniorrhaphy

A defect in the connective tissue of the abdominal wall is commonly referred to as an abdominal wall hernia. Intestines can protrude through this defect into a subcutaneous pocket, leading to discomfort and possibly bowel obstruction [4]. Hernias can occur at any weakened spot in the abdominal wall but are most seen in the linea alba (the midline) and the inguinal area. Abdominal wall hernias generally require surgical repair [4]. Unfortunately, up to 30% of patients require revision surgery due to infection, pain, or recurrence [5].

Different herniorrhaphy techniques have been developed, but literature is inconclusive on the best approach. Much is still unknown about the factors involved in unsuccessful outcomes. Surgical factors such as unwanted reactions between the host tissue and mesh implant, the applied closure technique, wound ischemia, and infection, combined with patient specific factors such as age, obesity, smoking, immune suppression, malnutrition, and diabetes are known to negatively impact the outcome of the surgery [2, 6, 7]. Additionally, excess tension in the abdominal wall may negatively influence surgical outcomes [8].

1.2. Problem statement

In ventral hernia repair, the aim is to close the defect, typically done by approximation of the aponeurotic edges and placing a mesh to support the site [9]. For the closure of the defect, the abdominal wall tension must be overcome. It is well known that excess tension at the aponeurotic edge during hernia repair may cause failure of the reconstruction followed by hernia recurrence [8]. However, there is no standardized objective method to quantify this tension. The choice of procedure relies on preoperative characteristics (e.g. hernia size) and surgical expertise [5]. Closure of the hernia defect is the main goal in hernia repair. If necessary, due to high tension, different adjuncts, such as component separation or intraoperative fascial traction, can be performed to aid closure. The assessment of safe closure is based on surgeon's assessment, which has been proven a very poor prediction [10].

Implementing objective tension measurement methods could supplement surgical expertise, aid in surgical decision-making, and ultimately reduce the recurrence rate. For open surgery, several methods to assess fascial tension exist. However, the same cannot be said for minimally invasive surgery. E.F. van Koten has presented a device capable of measuring abdominal tension [11], but its complexity prevented its introduction into the operating room (OR).

1.3. Research objective

The goal of this research is to design a device for use in laparoscopic herniorrhaphy to provide intraoperative information on fascial tension to the surgeon. Knowledge of the magnitude of fascial tension can help objectively assess the hernia and could provide insight into the most appropriate procedure for the best possible outcome. To achieve this, the work of E.F van Koten is used as a starting point, as she described a first concept of a minimally invasive tensiometry device (MINT). This thesis work includes:

- Identifying the drawbacks in the design by E.F. van Koten. (Chapter 4)
- Analyzing solutions to overcome these drawbacks. (Chapters 5 and 6)
- Integrating these solutions into a concept design. (Chapter 7)
- Evaluating the design with regard to the preset requirements. (Chapter 8)
- Presenting a safe and effective solution with a working prototype. (Chapter 10)

2

Background

Abdominal wall hernia repairs are among the most frequently performed general surgeries worldwide, and the MINT device could be of great interest in these procedures [1]. This chapter provides a medical background on this type of surgery and summarizes the first concept of the MINT as described by E.F. van Koten [11].

2.1. Anatomy of the abdominal wall

The abdominal wall is a complex, heterogeneous structure designed to contain and protect the abdominal viscera. It supports upright posture, limb movement and respiratory function [12]. It consists of multiple overlapping layers, including (from superficial to deep) the skin, subcutaneous tissue, muscles encompassed by fascia, and the peritoneum (Figure 2.1) [5, 13]. The two central vertical rectus abdominis are connected to a triple layer or flat muscles extending laterally. These muscles encompass the abdominal cavity and must withstand pressures generated internally whilst performing their functions [14]. The linea alba is an aponeurotic structure that runs vertically along the midline of the ventral abdominal wall and splits the left and right abdominal wall muscles, allowing for independent movement on each side of the abdomen [15]. It is formed by the interlacing of the aponeurotic fibers of the three lateral abdominal muscles. Although the linea alba is a strong structure, it is a common site for hernias.

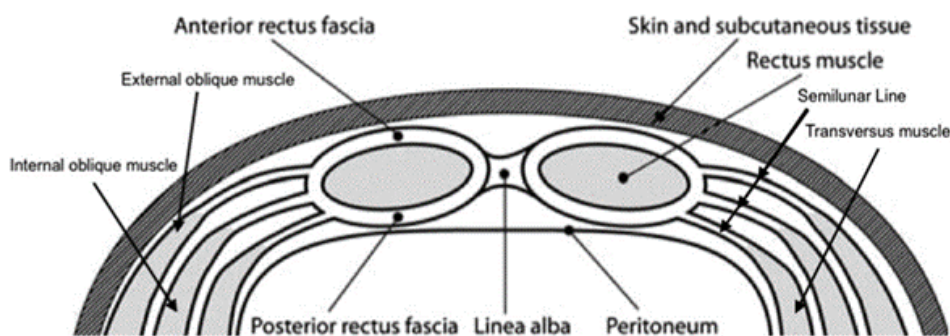


Figure 2.1: A cross-sectional diagram showing the anatomy of the abdominal wall [16].

2.2. Abdominal wall hernia

An abdominal hernia is an abnormal protrusion of intra-abdominal contents through a defect in the connective tissue of the abdominal wall without penetrating the skin, appearing as a visible bulge (Figure 2.2) [17, 18]. Abdominal wall hernias can occur at any weakened spot of the abdominal wall, such as the linea alba [13]. They can lead to discomfort and intestinal obstruction [18].

Abdominal wall hernias are categorized into two types: primary hernias, such as umbilical, inguinal,

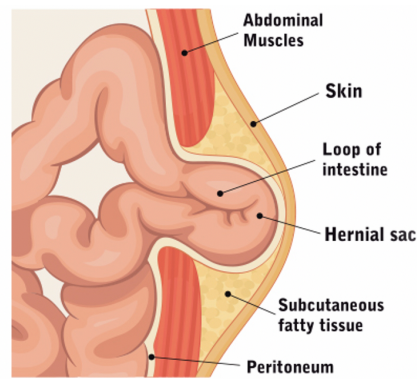


Figure 2.2: Protrusion of intestines in an abdominal wall hernia [4].

epigastric and Spigelian hernias, found at natural weak spots; and secondary hernias, which occur at weakened spots due to surgery, including incisional and parastomal hernias [13]. Most hernias require surgery to close the defect. In these, so called, herniorrhaphies the defect is closed by approximation of the aponeurotic edges and a mesh may be placed to support the abdominal wall reconstruction [9]. Recurrences are common, with estimated revision surgery rates ranging of 24% to 43% for ventral hernia repairs [3, 14].

2.3. Ventral hernia repair techniques

In ventral hernia repair, the aim is to close the defect, typically done by approximation (medialization) of the aponeurotic edges and placing a mesh to support the site [9]. Various hernia repair techniques exist and the surgeon decides which to use based on preoperative data, expertise and intraoperative findings, which may limit options due to prior damage to tissues.

Minimally invasive approaches (laparoscopic and robotic) for herniorrhaphy show lower infection rates, earlier discharge from hospital and shorter recovery times compared to open surgery whilst not impairing the chance of recurrence [14]. Additionally, patients undergoing laparoscopic surgery have a lower chance of developing incisional hernias postoperatively [15]. However, not all mesh placement locations can be reached laparoscopically.

In most cases a mesh is implanted in the abdominal wall to provide additional support which significantly reduces recurrence rates. In aim of reducing complications, a safe, strong, minimally inflammatory, integrative and infection and adhesion resistant mesh has been sought. Three classes of mesh have evolved: synthetic, composite, and biological. Various synthetic materials have been used for meshes, with Polypropylene (PP) being the most used. Different thicknesses exist for different applications. All PP meshes generate a foreign body response and produce a strong repair through rapid integration into the abdominal wall. Composite meshes have two different sides or use coatings to provide a barrier against adhesion. Biological meshes are commonly promoted in a contaminated field due to their ability to resist infection [14].

A mesh can be placed in every layer of the abdominal wall. Recurrence and complication rate differ between the different layer of implantation (Figure 2.3).

2.4. Clinical importance

Hernia recurrence necessitates revisional surgery in approximately one in three patients, incurring substantial costs in terms of pain, disability, time off work and procedural expenses [3]. Reducing the recurrence rate after ventral hernia repair would improve the expected quality of life and generate procedure cost savings (\$32 million annually in the United States per 1% reduction in recurrence rate) [14].

Current literature extensively discusses the type of mesh and placement of the mesh, while little to no research addresses the influence of the abdominal tension in minimally invasive ventral hernia repair. To date, fascial tension is subjectively assessed by the surgeon, although it is believed that fascial tension plays a role in the recurrence of abdominal wall defects. Due to the lack of evidence regarding fascial

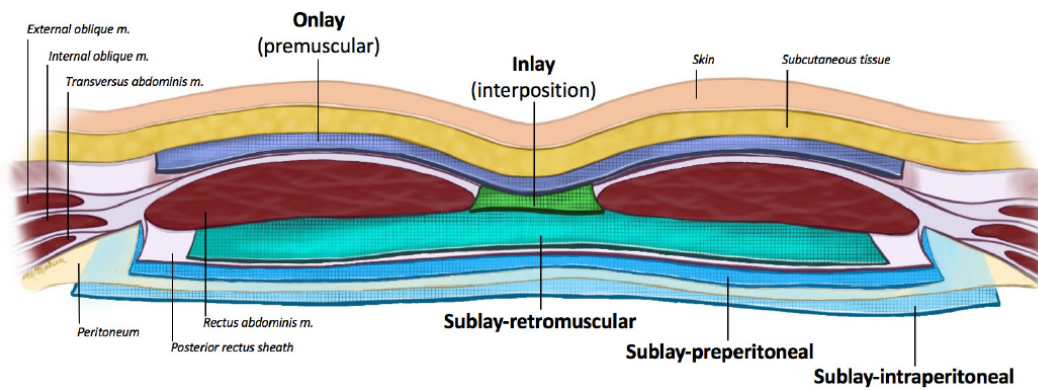


Figure 2.3: Mesh placement options [9].

tension and its correlation to postoperative success, surgeons rely on their own experience to determine the closing method.

Obtaining objective intraoperative measurements of the fascial tension could provide valuable data to assist surgeons in their decision-making. As of today, no medical devices to objectively assess the fascial tension to provide surgeons with this useful intraoperative data exist.

2.5. MINT by E.F. van Koten

E.F. van Koten has attempted to develop a medical device to provide surgeons with an objective measurement of the fascial tension [11]. This thesis is a follow-up on the work by E.F. van Koten, who laid the foundation for this thesis by discussing various methods to quantitatively assess abdominal wall tension. She determined that a purely mechanical force sensor using a linear spring scale combined with a distance measurement would be best suited for this application which led to the device illustrated in Figure 2.4a. The device, named MINT (Minimally INvasive Tensiometry), comprises a main body and thirteen separate parts (Figure 2.4b). The device can be attached to the handle of a laparoscopic forceps. Then, by pulling on the handle of the MINT, a force measurement can be performed whilst the traveled distance is measured with a ruler. The entire device must be disassembled for sterilization and must be reassembled for each surgery. This process, which requires an Allen wrench, was found to be tedious and prone to losing components. Therefore, this design was not yet ready for implementation. This thesis aims to design an improved version of this original MINT, containing a linear spring scale, which will retain the same name.



(a) The assembled MINT by E.F. van Koten [11].

(b) The separate components of the MINT by E.F. van Koten [11].

Figure 2.4: An overview of the design by E.F. van Koten.

3

Methods

This chapter gives an overview of the design process and the structure of the thesis.

3.1. Design process

The project revolves around the improvement of the design of the MINT as designed by E.F. van Koten. This device allows surgeons to quantify abdominal wall tension during minimal invasive surgery (MIS). To make an optimal design for these surgeons, their opinions and suggestions have been considered throughout the entire design process. Due to this feedback, the process became highly iterative.

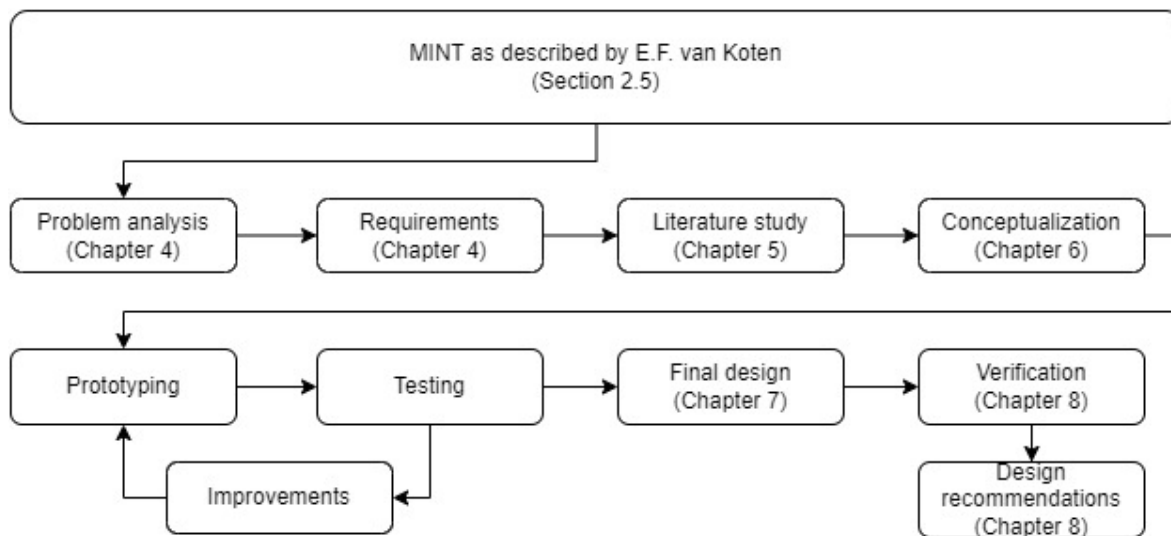


Figure 3.1: Flowchart displaying the design process.

3.2. Thesis structure

This thesis is structured around the design process as shown in Figure 3.1. This design process is the continuation of the design project by E.F. van Koten which is used as the starting point of this project. A summary of this design is provided in Section 2.5. For a more detailed explanation of her design process, her thesis should be consulted [11].

Chapter 4: Problem Analysis

A problem analysis was performed to find out why the MINT as described by E.F. van Koten is not yet implemented. It was found that the high component count and the size of these components hindered the implementation. Reducing these factors would greatly benefit the MINT and therefore became the

research objective. This chapter also states design requirements where safety and an effective design were considered priorities.

Chapter 5: Literature study

A literature study was conducted to explore potential solutions for improving the MINT. It was found that most of the components were used for forming the connection between the MINT and the laparoscopic forceps. Therefore, a systematic patent review was performed to gather insights and inspiration for a new connection mechanism. The study revealed that moving away from the original C-clamp design in favor of a male-female connection is the most promising approach.

Chapter 6: Conceptualization

The conceptualization phase has proven to be the most creative phase in this process. The three main functions of the MINT (connection, force measurement and distance measurement) were thoroughly explored, with various approaches considered for each function. For each function, several solutions were formulated, and prototypes have been produced. Clinical and technical experts were included in the evaluation of these concept solutions to gather feedback that could be used in the various iteration cycles.

Chapter 7: MINT-Final Design

Multiple iterations were conducted before reaching the final design. This new, more simplistic, MINT comprises only five components and does not require any tools for assembly. A final prototype was made for verification.

Chapter 8: Verification

The final prototype was verified for compliance with the requirements with a variety of tests. These tests include evaluating the accuracy of the force gauge and sterilization tests. Additionally, the assembly and disassembly time were assessed, and a finite element analysis was performed.

4

Problem Analysis

It is believed that quantifying abdominal wall tension can function as a feasible adjunct to surgical decision making during herniorrhaphy. However, as of today, no methods to minimally invasive quantify abdominal wall tension exist. An attempt was made by E.F. van Koten in 2021. This device can be attached to a laparoscopic instrument and perform a force measurement and a distance measurement. However, her device has not been implemented due to several reasons all originating from the components in the device. This chapter will analyze these downfalls, will formulate the research objective and the requirements for the "new" improved MINT.

4.1. Components

The MINT designed by E.F. van Koten entailed two main problems: the number of components and the size of the components.

4.1.1. Number of components

The original MINT comprises fourteen components. The parts have been grouped based on their functionality in Figure 4.1. These components must be disassembled during the cleaning and sterilization process and have to be assembled in the OR during the surgery. For this an Allen wrench is required which also needs to be reprocessed before each surgery.

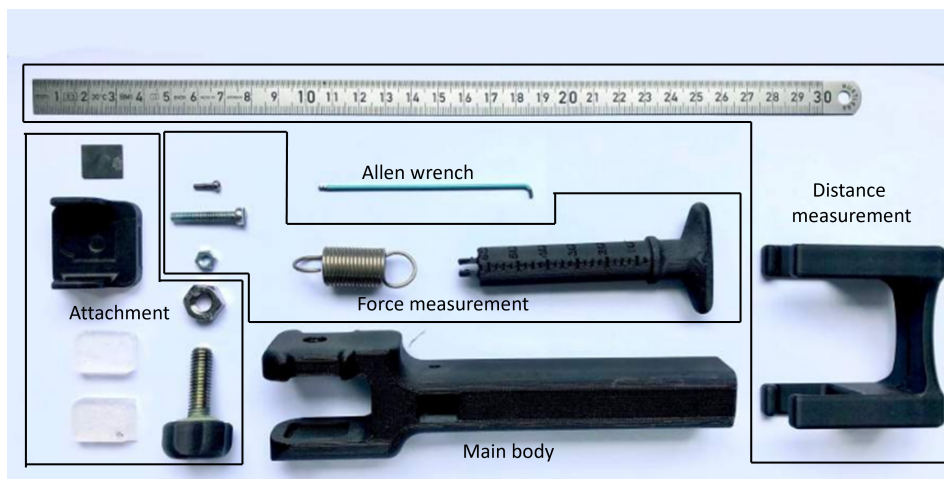


Figure 4.1: Components of the original MINT grouped based on their function within the device. The Allen wrench is not part of the device, however it is required for the assembly of the device. (Adapted from E.F. van Koten [11])

This high number of components complicates the implementation of the device in two ways. The number of components results in a longer assembly time in which the assistant can not perform

other tasks.

Additionally, according to the DSMH (an expert on sterile medical devices) at the Reinier de Graaf Gasthuis (RdGG), this high number of components also complicates the sterilization process as it is hard to keep all components together. Thus, by following Murphy's law "Anything that can go wrong, will go wrong.", it is likely that at some point incomplete devices will be delivered to the OR. This would make the use of the device impossible, or, if surgeons still use the device, dangerous.

4.1.2. Size of the components

Another aspect of the components that complicates the implementation of the device are the small components. These complicate the implementation in two ways.

The assembly of the device takes place in a sterile environment. Therefore, the person assembling the device wears sterile gloves. The small components are hard to handle and make the assembly tedious and time consuming.

Additionally, the sterilization process is complicated by the small components as they are transported, cleaned, and sterilized in medical instrument trays. The bottom of these trays is made of a metal mesh to allow water to flow through the tray (Figure 4.2). Three components and the Allen wrench have proven to be able to fall through the holes in the tray (Figure 4.3). This could result in incomplete sets if it happens during transportation to the sterilization department or during the cleaning process. If the components fall through the mesh during or after the sterilization process, the sterile cloth could be damaged. If this happens, all components within that tray are considered non-sterile. This means that the MINT and the other devices within that tray cannot be used in the surgery.



Figure 4.2: A medical instrument tray [19].

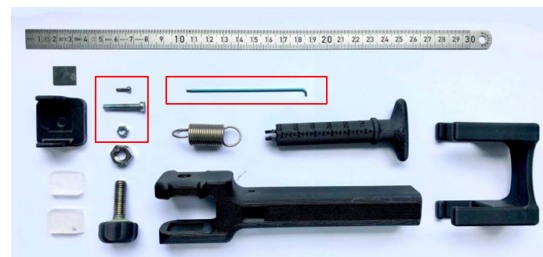


Figure 4.3: Components of the original MINT. The three components and the Allen wrench within the boxes could fall through the mesh of the instrument tray. (Adapted from E.F. van Koten [11])

4.2. Research objective

The ultimate goal of the MINT is enabling surgeons to obtain intraoperative quantitative data which helps with decision making during the surgery on order to improve patient care. To implement the MINT in this medical context, the two previously mentioned drawbacks of the device must be overcome. Therefore, this research aims to design an improved MINT which overcomes these two drawbacks by focusing on minimizing the number of components.

4.3. Requirements

The reduction of the number of components is required for the implementation of the MINT, however this reduction may never compromise the safety (both for the patient and OR-personnel). The current MINT comprises fourteen components and requires one tool for assembly. It was chosen to aim for a reduction of 50%. This resulted in aiming for eight components (including optional assembly tools) in the new design.

Additionally, the original functions of the MINT must be preserved in the new design. These functions include measuring the applied force and measuring the traveled distance in the medialization of the hernia.

Additionally, the MINT should be able to be implemented in Europe. This means that the MINT should obtain a CE-mark. Having a low-risk device eases the process of obtaining a CE-mark and thus the device is designed to be a Class I device.

Table 4.1: Device requirements

The device must	The device should	The device should not	The device must not
Be safe to use (both for the OR-staff and the patient).	Have less than eight components.	Have small components which could fall through the gauze of the sterilization basket.	Damage or compromise the laparoscopic forceps.
Be able to measure the force required to medialize the hernia (maximum 50 N with an accuracy of ± 3 N).	Have an assembly time faster than two minutes.	Extend more than 20 cm behind the laparoscopic forceps.	Contain parts that should or could be introduced into the trocar or the body.
Be able to withstand 1000 sterilization cycles.	Have a clear readability.	Exceed 6 cm in width.	
Be able to measure the distance (maximum 10 cm with an accuracy of ± 2 mm).	Be compatible with a diversity of laparoscopic forceps.		
Be attachable to a laparoscopic forceps whilst withstanding a pulling force of 50 N.	Allow for calibration each year.		
Be able to be assembled by OR-staff wearing sterile gloves.	Allow the measurements to be taken within 5 minutes.		
Be operable by a single surgeon.	Weight less than 1 kg.		
Be operable by surgeons with hand sizes above a size 6.	Be able to apply for a CE mark as a Class I medical device.		

These and other requirements are listed in Table 4.1. These requirements are based on the thesis of E.F van Koten and further supplemented with expert wishes. In this table the requirements are sorted in four groups. These groups are defined as follows;

- **Must:** Essential requirements that must be absolutely fulfilled for the product to function safely and as intended.
- **Should:** Important but not essential requirements. Failure to meet these requirements will not result in unacceptable risks.
- **Should not:** Activities or characteristics that are strongly discouraged but not strictly forbidden.
- **Must not:** Activities or characteristics that are prohibited as they could compromise the safety.

The requirements were kept in mind during the entire design process to ensure a safe and effective design. Additionally, in the verification step of the process, the requirements were used to verify the final design (Chapter 8).

5

Literature Study

Prior to the conceptualization phase, a literature study was conducted in order to provide a systematic overview of patented connecting mechanisms that could be used as a source or inspiration for the connecting mechanism of the MINT. It was chosen to focus on the connection mechanism as this is the function requiring the most components in the original MINT; six out of fourteen components (see Figure 4.1). In this chapter a concise summary of this study will be given. For a more detailed explanation the patent study may be consulted [20]. The patent study identified five different groups of connecting mechanisms:

- (A) Friction-based clamping with a bolt acting directly on the to be fixated component
- (B) Friction-based clamping with a bolt which does not act directly on the to be fixated component
- (C) Friction-based clamping without the use of bolts
- (D) Connecting based on male-female components
- (E) Other connection methods

Conceptual drawings of these categories can be found in Figure 5.1. Group E is not included in this representation due to the extensive diversity among the patents.

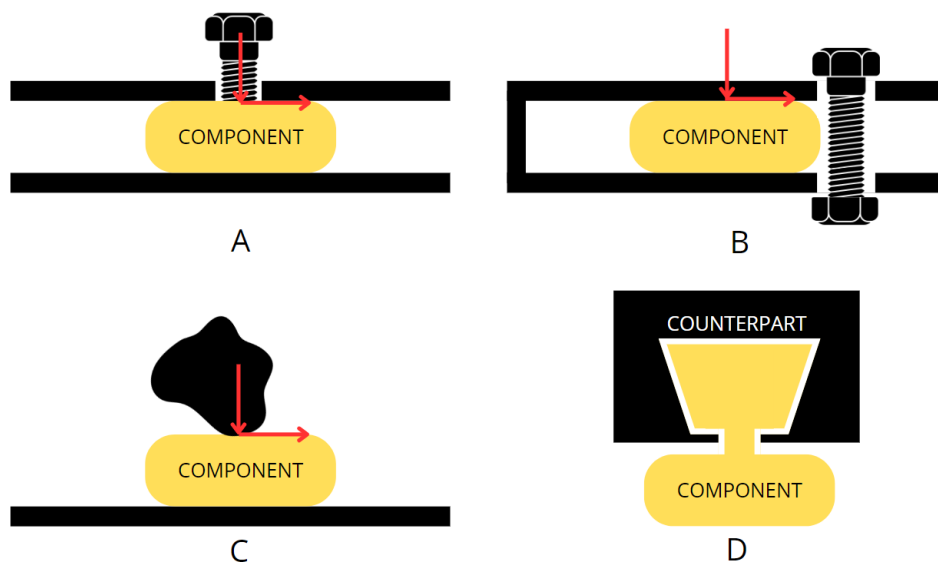


Figure 5.1: Schematic representation of the connection principles of group A, B, C and D.

These groups were analyzed based on their component count and on whether they are likely to

Table 5.1: Harris profile assessing the five identified connecting mechanism groups.

	Group A				Group B				Group C				Group D				Group E			
	--	-	+	++	--	-	+	++	--	-	+	++	--	-	+	++	--	-	+	++
Number of components																				
Bending moment	■	■			■	■	■	■	■				■	■	■	■	■	■	■	■

introduce a bending moment to the laparoscopic forceps when implemented. These analyses have been summarized in a Harris profile shown in Table 5.1.

The connection mechanism in the MINT as described by E.F van Koten would be categorized as a category A mechanism. This category has a relatively high number of components compared to the other categories and also shows a tendency of introducing a bending moment. This results in relatively low scores in the Harris profile. In contrast to category A, category D shows relatively high scores on both criteria, suggesting that these mechanisms would better suit this application. Therefore, it was chosen to redirect research on the connecting mechanism of the MINT towards male-female connection mechanisms.

6

Conceptualization

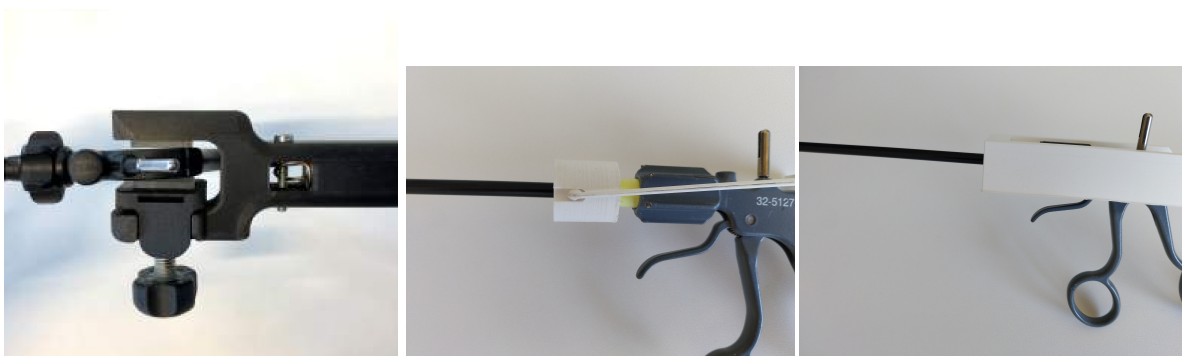
In the conceptualization phase of the project, several concept solutions have been considered. In a design comprising a linear spring, three main functions can be distinguished;

- The attachment of the main body to the laparoscopic forceps (Section 6.1)
- The mechanical force gauge (Section 6.2)
- The distance measurement (Section 6.3)

These three functions will be discussed in the following sections.

6.1. Connection between laparoscopic grasper and MINT

As mentioned in Chapter 5, the MINT as described by E.F. van Koten uses a bolt to fasten the MINT to the handle of a laparoscopic forceps (Figure 6.1a). To be able to reduce the number of components, this study focuses on male-female connection mechanisms. Two distinct options to attach the MINT to the shaft of the laparoscopic forceps have been found. The first being the usage of a small cylindrical coupler block which is slid onto the laparoscopic shaft to form an attachment site for the main body (Subsection 6.1.1). The second being a version in which these two components are integrated into one component. In this construction the whole main body is slid over the laparoscopic shaft (Subsection 6.1.2). Several options in which the MINT is attached to the handle of the laparoscopic forceps have also been explored. However, due to the variability of the handles, these options were not feasible.



(a) Top view of the connection mechanism used in the design by E.F. van Koten [11]. (b) Side view of a connection mechanism with a cylindrical coupler block. (c) Side view of a connection mechanism with an incorporated coupler piece in main body.

Figure 6.1: The three different connection mechanisms discussed in Section 6.1.

6.1.1. Cylindrical coupler block

The first explored option revolves around a male-female coupler block as seen in Figure 6.1b. This cylindrical coupler block has a cylindrical hole in the center and two recesses at either side of the

cylinder. A connection between the laparoscopic forceps and the device can be made by sliding the cylindrical coupler block over the shaft. This block in turn acts as the connection site for the main body which has protrusions that can interlock with the recesses at either side of the coupler block.

6.1.2. Integrated coupler piece in main body

In aim to reduce the number of components even further, it could be opted to permanently attach the main body to the coupler block. This would result in one large main body with a cylindrical hole in the front through which the laparoscopic shaft can be introduced (Figure 6.1c). By integrating the two components into one body, a more sturdy and reliable connection can be made. Additionally, it brings the component count down by one.

6.1.3. Choice of connecting mechanism to the laparoscopic forceps

The cylindrical coupler block option could ease the procedure as the block can stay attached to the laparoscopic forceps throughout the whole procedure without compromising the range of motion of the forceps. Therefore, mounting the main body to the forceps can be done quick and whilst the forceps is already holding the fascia on which the measurement will be performed. The other connection option, in which the coupler piece is integrated into the main body, does require the forceps to be taken out of the patient during attachment to the forceps before the fascia can be grasped. Therefore, this method would require some additional time.

This additional time was justified by surgeons as they found the option with the cylindrical coupler block to feel "flimsy" and they prefer the sturdier integrated version. Therefore, it was chosen to incorporate the method in which the coupler piece is integrated into the main body in this design.

6.2. Mechanical force gauge

The mechanical force gauge is the part of the MINT which allows the user to quantify the pulling force exerted on the fascia. It consists of a spring and a straight guide. Options with two springs on either side of the laparoscopic handle were also considered in aim of decreasing the length of the device. However, the increase in complexity could not be justified by the marginal reduction in length.

6.2.1. Spring

The same linear spring as used by E.F. van Koten will be used in this design [11]. This spring is manufactured by Tevema. The specifications of the spring provided by the manufacturer are listed in Table 6.1. This linear spring has a pretension and thus Hooke's law should be adapted to account for this factor (Formula 6.1).

$$F = F_0 + C * \delta \quad (6.1)$$

Table 6.1: Spring specifications provided by the manufacturer [21].

Variable	Value
Product number	T42010
Spring constant, C	0.94 N/mm
Pre-tension, F_0	5.52 N
Max force, S_n	65.26 N
Initial length, L_0	43.30 mm

After mechanical testing of the first concept design, large errors were found in the force gauge. This led to questioning the specifications provided by the manufacturer. Mechanical testing of the spring confirmed this suspicion. In this test, the spring was vertically suspended in air. Different masses were added to the lower end of the spring and the deflection was measured using a caliper. The least square error method was used to estimate the spring constant and the pretension ($C = 0.8397$ N/mm and $F_0 = 2.172$ N). The data of this test can be found in Appendix A. The reason of the difference between these values and the values provided by the manufacturer was not investigated and seen as not within the

scope of this research. However, explanations could be plastic deformation due to abuse of the spring or a manufacturing error as errors were also apparent in the design by E.F. van Koten [11].

6.2.2. Connection between main body and the spring

Two options to connect the spring to the main body were considered. Both options are shown in Figure 6.2. The first option (Figure 6.2a) introduces a connection piece from the top whereas the second option (Figure 6.2b) introduces the connection piece from the side. The second option was preferred as this connection piece was found to be more secure and intuitive compared to the first option.

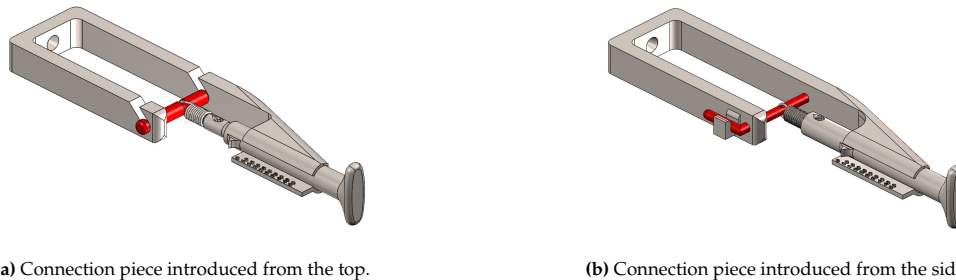


Figure 6.2: The two considered connection options to connect the spring to the main body of the MINT. In both figures, the connection part is indicated with a red color.

6.2.3. Straight guide

A straight guide was implemented for three reasons.

The straight guide provides a housing for the handle and thereby holds every component in place, making operation of the device easier and components can no longer fall after assembly.

Additionally, by adding the straight guide, the pulling force is always in line with the laparoscopic forceps, minimizing errors that could occur.

And finally, can this straight guide also be used to hold the measurement scale of the force gauge. It was chosen to place the measurement scale on the main body instead of the handle (as done by E.F van Koten) as this allows the surgeon to always see the whole scale. This allows them to better estimate the true value. The next example, in which the true value would be 18 N, provides an insight into this claim. When placing the scale on the handle the surgeon would only know that the value is higher than 10 N but not really to which extend because he is not able to see the 20N-mark (see Figure 6.3a). Placing the scale on the straight guide (as done in Figure 6.3b), allows the operator to see the whole scale and could thus see that the value lies between 10 and 20 N but slightly more to the 20 and could thus make a more educated guess of 18 N.



(a) Force scale placed on the handle as done by E.F. van Koten.

(b) Force scale placed on the straight guide.

Figure 6.3: Two possible force scale placements. Both figures indicate a force of 18 N.

6.3. Distance measurement

Besides the force, also the traveled distance during the medialization of the hernia is considered of importance as this allows for the translation from force to tension. This could be done by placing a ruler inside the abdominal cavity, however it is preferred to not introduce additional objects in the abdominal cavity. As shown in Figure 6.4, is the traveled distance of the hernia the same as the difference in distance from the handle of the laparoscopic instrument to the trocar. This means that this measure could be used to quantify the traveled distance of the hernia. The following section provides an overview of six different concept solutions. These concepts have been weighed against the criteria set in Subsection 6.3.2.

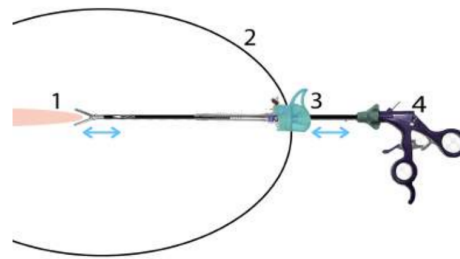


Figure 6.4: Schematic drawing of the displacement of the abdominal wall defect (1 = abdominal wall, 2= abdomen, 3= trocar, 4= laparoscopic instrument) [11].

6.3.1. Concept solutions

The six concept solutions have been visualized in Figure 6.5. In these drawings the main body is indicated in gray whereas the black components with arrows indicate moving components. Explanations of these concept solutions can be found in the following sections.

Concept 1

This solution uses a movable ruler that can slide along the main body of the MINT. Measurements can be taken by placing the tip of the ruler against the trocar and then placing a finger, a piece of tape or a dot on the main body where the zero of the ruler is at. When the fascia is put under tension and the MINT has moved backwards, the tip of the ruler is once again placed against the trocar. The value that is at the finger, the piece of tape or dot is the value corresponding to the traveled distance.

Placing tape could leave residual glue and dots placed by a pen might also leave residual matter. Therefore, the reusable option, by placing a finger, is considered in the evaluation.

Concept 2

The second solution involves a movable ruler placed in a movable holder with an arrow. Measurements can be taken by placing the tip of the ruler against the trocar and then moving the movable holder such that the arrow indicates the value zero. When the fascia is put under tension and the MINT has moved backwards, the tip of the ruler is once again placed against the trocar. The value that is indicated by the arrow is the value corresponding to the traveled distance.

Concept 3

The third solution involves a movable ruler that can slide along the body of the MINT. An indicator is permanently placed on the main body of the MINT. Measurements can be taken by placing the tip of the ruler against the trocar. The value at the location of the indicator should be remembered or written down. When the fascia is put under tension and the MINT has moved backwards, the tip of the ruler is once again placed against the trocar. The remembered or written down value should then be subtracted from the new value at the indicator to obtain the traveled distance.

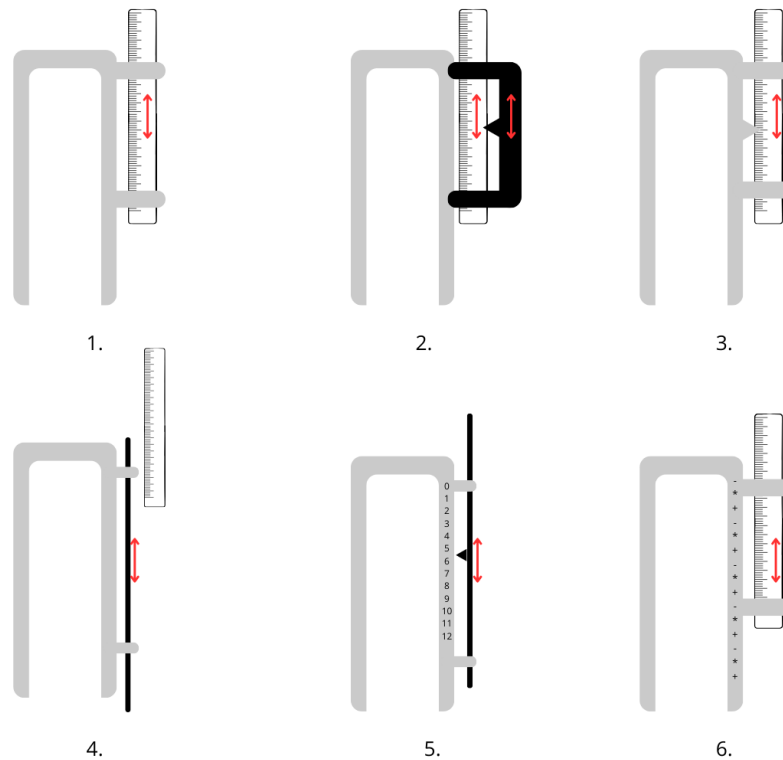


Figure 6.5: The six concept solutions for measuring the travelled distance. The numbers under each concept correlate to the numbers of the concept explanations.

Concept 4

The fourth solution uses a movable thin rod and a separate ruler. Measurements can be taken by placing the tip of the thin rod against the trocar. When the fascia is put under tension and the MINT has moved backwards, the traveled distance can be measured with the ruler as this is the distance between the tip of the rod and the trocar.

Concept 5

The fifth concept uses a ruler permanently placed on the main body of the device in combination with a movable thin rod with an indicator attached. Measurements can be taken by placing the tip of the thin rod against the trocar. The value at the location of the indicator should be remembered or written down. When the fascia is put under tension and the MINT has moved backwards, the tip of the thin rod is once again placed against the trocar. The remembered or written down value should then be subtracted from the new value at the indicator to obtain the traveled distance.

Concept 6

The last concept solution uses a movable ruler that can slide along the main body of the MINT. Multiple indicators, such as letters or symbols, are placed on the main body. Measurements can be taken by placing the tip of the ruler against the trocar. The indicator (the letter/symbol) that is the closest to 0 should be remembered. When the fascia is put under tension and the MINT has moved backwards, the tip of the ruler is once again placed against the trocar. The value on the ruler that now is at the remembered indicator (letter/symbol) is the value corresponding to the traveled distance.

MINT - Final Design

Several iteration cycles have been completed before finalizing the design of the MINT (Figure 7.1). The various aspects of the design will be elaborated on in the following sections.



Figure 7.1: Isometric drawings of the final design.

7.1. Design

The final design consists of five components, all serving their own purposes. The five parts are visualized in Figure 7.2 and technical drawings of the main body, the handle, the L-shaped link and the distance indicator are provided in Appendix C.

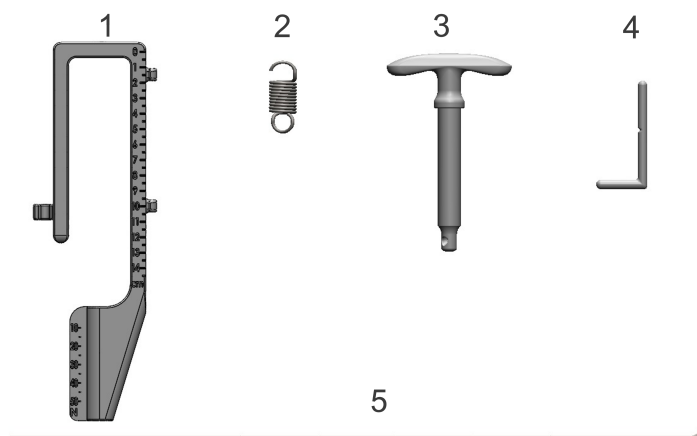


Figure 7.2: The five components of the final design; 1) Main body 2) Spring 3) Handle 4) L-shaped link 5) Distance indicator.

The main body serves as the connection mechanism as well as the housing for all the other components. The U-shaped front allows for insertion of laparoscopic forceps with a handle width up to 40 mm. On the sides of the main body three protrusions are mounted. The protrusion on the left side serves as a locking mechanism for the L-shaped link and the protrusions on the right side hold the distance indicator.

The L-shaped link allows for a secure connection of the spring to the main body. It is introduced from the left side of the main body and is locked in place by turning it into the protrusion on the side of the main body.

The handle serves several purposes. Firstly, it is the place where the operator holds the device whilst performing the measurements. Compared to the handle of E.F van Koten, the handle is rotated 90° to reach a vertical position. This position provides a more ergonomic environment for the operator's wrist. Additionally, it was opted to make the handle concave opposed to convex and twice as wide as the original handle (see Figure 7.3). This change allows for operation of the device by surgeons with larger hand sizes and minimizes the chance of the handle slipping out of the operator's hands (confirmed by two surgeons with glove sizes 7½ and 9).

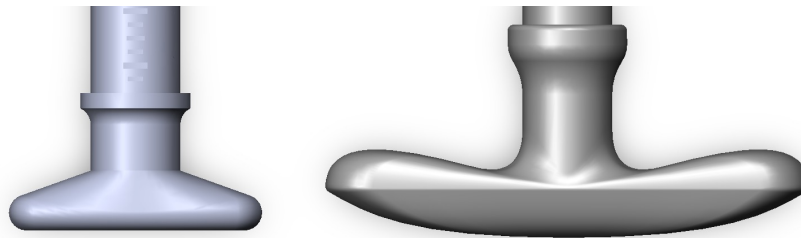


Figure 7.3: The handle of the original design of the MINT by E.F. van Koten (left) and the handle of the final design (right).

Besides being the holding site, the handle also acts as the force measurement indicator. For this an arrow was placed at the anterior side of the handle which points towards the Newton scale on the straight guide of the main body. A bulge is used on the posterior end to prevent the handle from going into the straight guide completely and ensures that all components stay connected.

The distance indicator is introduced through the two protrusions at the right side of the main body. This distance indicator can slide and notches in the indicator can be used to determine the medialized distance of the hernia. The anterior end is bent to allow for easier manipulation of the distance indicator. Additionally, this increases the contact area of the indicator on the abdominal wall further decreasing the chance on inducing trauma to the abdominal wall.

7.2. Materials and manufacturing

In this design three materials can be found, and several manufacturing methods are used.

The main body, the L-shaped link and the handle are all made of polyamide 12 (PA-12) and are produced by Oceanz [22]. This company is ISO 13485 certified to produce reusable sterile medical devices from this material. This material shows great mechanical properties whilst having a relatively low mass density ($\rho \approx 1.01 \text{ g/cm}^3$ [23]). This allows the whole device to be 164 grams (SS316 for these parts would make the mass approximately seven times higher). It was chosen to use 3D-printing for these components as they pertain some features that could not be manufactured using traditional manufacturing methods. The 3D-printing method used is selective laser sintering (SLS). SLS builds objects, layer by layer, by fusing or sintering areas of powder using thermal energy supplied through a laser beam [24].

The distance indicator is made of stainless steel AiSi 316. This stainless steel has great corrosion properties. This component can be manufactured from a solid 3 mm diameter rod. For this, first chamfers are added to the ends to ensure that no sharp edges exist on the final design. Then notches are made that act as the indicators and which are placed 50 mm apart to allow for measurements independent of the hernia placement. Then one end is bent 90° to form the handle of the distance indicator.

The spring in the new MINT is the same as the spring in the original MINT by E.F. van Koten. This spring is store bought and made of stainless steel 302.

7.3. Procedure

The MINT will be used to assess the fascial tension during ventral hernia repair. For this, the surgeon will prepare the tissue for closure in an equivalent manner to the current surgery. During this, the sterile OR-assistant assembles the MINT and attaches it to a laparoscopic forceps according to the instruction manual (see Figure 7.4). For use, the surgeon grasps the fascia with the laparoscopic gripper. Then, the surgeon places the anterior end of the distance indicator on the skin of the patient or against the trocar. Then force will be applied on the defect by pulling on the handle, medializing the edge of the defect. The protrusion on the handle of the MINT will indicate the applied force. To obtain the value of the medialized distance of the fascia, the distance indicator is once again placed against the skin of the patient or the trocar. The difference between the first distance measurement and the second distance measurement will correspond to the traveled distance of the fascia. This data will be gathered for future research. The MINT will be detached, and the surgeon can proceed with the surgery according to their judgment, taking the measurement results into account when guidelines have been formulated. A more detailed explanation of the assembly, disassembly, and use can be found in the instruction manual of the MINT which is provided in Appendix D.



Figure 7.4: MINT mounted on a laparoscopic grasper.

7.4. Costs

Two estimations on the production costs have been made. The first estimation is based on the production of one single device (Subsection 7.4.1). The second estimation is based on the production of 100 devices (Subsection 7.4.2). A 21% tax is included in both estimations.

7.4.1. One device

The estimated production costs of one single device are €355.73. A summary of the expenses can be found in Table 7.1.

In this list, the costs of the main body, the handle and the L-shaped link are combined in the item "3D printed parts" as they are all 3D printed. The costs are based on quotations of manufacturer Oceanz. The costs for the spring of Tevema include shipping costs and a control chart. The shipping costs with this manufacturer are €20.00 independent of the number of ordered components. The control chart is a service provided by Tevema in which they check all springs for their parameters. This is not required for the MINT, however it is advised to have the spring checked as this minimizes the chance of errors in the force measurements.

The costs of the distance indicator include the material costs for the distance indicator (AlSi 316, 3 mm \varnothing , 450 mm), labor and shipping costs [25]. The labor costs of this part is estimated based on the following assumptions. Firstly, it was assumed that the production time of one single distance indicator is 30 minutes. Secondly, a workshop hourly rate of €100.00 was assumed. This results in €50.00 labor cost of this single component.

Table 7.1: Production costs of one device.

Component	Cost item	Costs (€)
3D printed parts (main body, L-shaped link and handle)	Parts	189.41
	Medical declaration of conformity	42.32
	Shipping	11.28
Spring	Spring	7.72
	Control chart	18.15
	Shipping	20.00
Distance indicator	Material	6.05
	Labor	50.00
	Shipping	10.80
Total		355.73

7.4.2. One hundred devices

A reduction in production costs per unit can be observed when more devices are to be made. In Table 7.2 a summary of the expenses for the production of one hundred devices can be found. A decrease in costs of the 3D printed parts can be observed. This is due to volume discounts provided by manufacturer Oceanz.

Furthermore, it can be seen that the labor costs of the distance indicator are lower compared to the labor costs for the production of a single device. This is due to a more serial production which increases the production speed to an estimated production of ten components per hour.

As can be seen, a reduction from €355.73 to €166.98 per device can be obtained by up-scaling the production.

Table 7.2: Production costs per 100 devices.

Component	Cost item	Costs 100 devices (€)	Costs per unit (€)
3D printed parts (main body, L-shaped link and handle)	Parts	15142.88	151.43
	Medical declaration of conformity	42.32	0.42
	Shipping	29.21	0.29
Spring	Spring	341.22	3.41
	Control chart	18.15	0.18
	Shipping	20.00	0.20
Distance indicator	Material	26.28	0.26
	Labor	1000.00	10.00
	Shipping	78.65	0.79
Total		16698.71	166.98

8

Verification

In this chapter, the design is evaluated for compliance with the requirements set in Section 4.3. For three requirements, more elaborate testing was required. These tests are elaborated on in Sections 8.1, 8.2 and 8.3. Additionally a finite element analysis was performed as shown in Section 8.4. A summary of the verification process can be found in Section 8.5.

8.1. Force measurement

As can be seen in Table 4.1, the device must be able to measure the force applied on the hernia with a maximum force of 50 N with an accuracy of 3 N. For this, a linear tension spring was used in combination with the measurement scale on the straight guide. To assess the accuracy of the force gauge on the device, a force test was computed. In this test a portable electronic scale (max mass: 40 kg, accuracy: 10 g) was placed in line with the MINT (see Figure 8.1). Measurements were taken by pulling the handle till it indicated the prescribed force (10, 15, 20, 25, 30, 35, 40, 45, 50 N). Then the corresponding value on the portable electronic scale was read. The data from this test can be found in Appendix E.1 and are more visually presented in Figure 8.2.



Figure 8.1: The setup used for the force measurements. The portable scale (right) is placed in line with the MINT while force is being applied to the handle of the MINT (left).

From this data can be seen that larger errors occur at higher forces. This can be the result of minor changes in specifications of the spring. This could be resolved by readjusting the force scale on the main body. Furthermore, larger differences in error between the four measurements exist at higher forces. The largest spread in errors were measured at 40 and 45 N with a difference between the highest and lowest measured error of 1.8 N, staying well underneath the allowed 3 N.

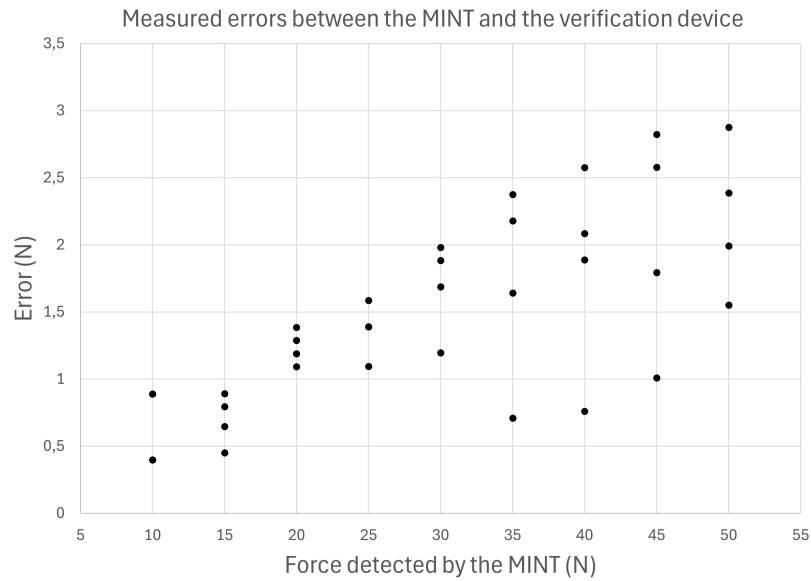


Figure 8.2: A visual representation of the measured errors in the force verification measurements.

8.2. Assembly and disassembly time

As can be seen from the requirements in Table 4.1, the assembly time of the device should be shorter than two minutes. To assess the assembly time, the device was assembled and connected to a laparoscopic forceps whilst the time was recorded with a stopwatch. Then, the device was completely disassembled following the steps listed in the user manual. These measurements were repeated ten times by each participant and were performed whilst seated at a desk and wearing gloves to simulate the operating room environment. It was chosen to include two participants; one who has never assembled/disassembled the devices before the test ("novice") and one who has done it multiple times before and did not need to read the instruction manual anymore ("expert"). The same test has been conducted with the original MINT (the MINT designed by E.F van Koten) and for both devices, the time measurements are listed in Appendix E.2. Both data sets are visualized in Figure 8.3.

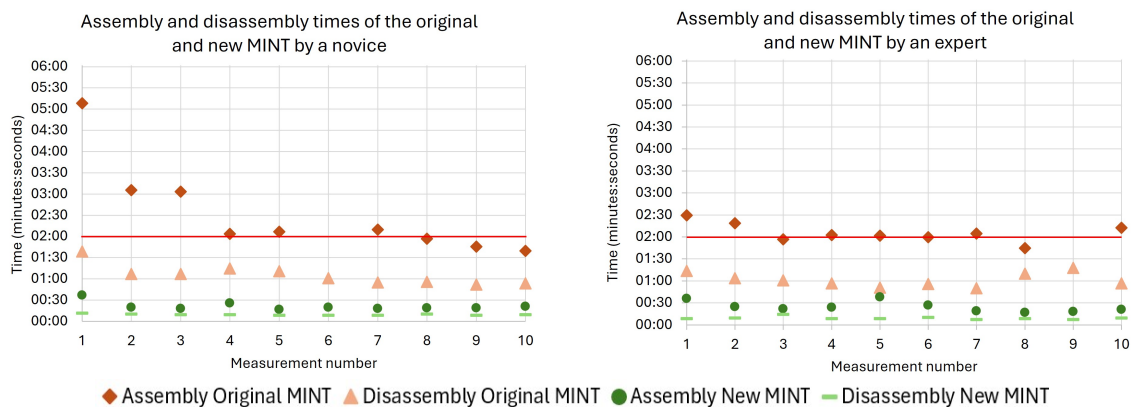


Figure 8.3: Visual representation of the measured assembly and disassembly times of the original MINT and the new MINT executed by the novice participant (left) and the expert participant (right).

From this data it can be seen that the time requirement of two minutes was only met five times by the original MINT and the mean assembly time was higher than two minutes for both participants. Additionally, the assembly of the original design was not completed two times due to components falling on the floor. If that happens in the OR, no measurements can be taken due to sterility reasons. Furthermore, unsafe situations were observed in the original design as the MINT was not

always connected properly to the laparoscopic forceps. In the OR, detachment of the device from the laparoscopic forceps could introduce dangerous situations.

The new MINT assembly time always stayed well under the two-minute mark with a mean assembly time of 21 and 24 seconds for the novice and advanced participant respectively. Additionally, a secure connection between the MINT and the laparoscopic forceps was obtained in all assemblies. Thus, no unsafe conditions were created or experienced.

The disassembly time is not restricted by the requirements but a substantial improvement in disassembly time was achieved by simplifying the design.

This test aimed to assess the assembly time of the new design of the MINT. For completeness also the old design and the disassembly time were included in this test. It was found that the new design meets the requirement "The device should have an assembly time faster than two minutes." Additionally, no unsafe situations were observed during the assembly and disassembly of the new design.

8.3. Steam sterilization

As the MINT will be used in a sterile environment aimed to minimize the chance on infections, it is important that the device can be sterilized without compromising its functionality. During the conceptualization phase attention was paid to a modular design so all parts can be sterilized separately. In this test only the sterilization step of the reprocessing process was investigated under the assumption that the device can be cleaned and disinfected without issues as the DSMH (an expert on sterile medical devices) of the RdGG foresees no problems in these steps. To assess this criterion, the device underwent ten autoclave steam sterilization cycles to observe possible deformations in the material. Table 8.1 shows the autoclave settings of these cycles. Between each cycle, the device was removed from the autoclave to cool down.

Table 8.1: Used sterilization program.

Item	Setting
Packaging	Unwrapped
Sterilization temperature	134 ° Celsius
Sterilization time	3.5 minutes
Sterilization pressure	2 bar
Drying time	10 minutes

After ten steam sterilization cycles, a slight deformation was observed in the main body of the MINT causing the two sides to become misaligned. As a result, the ends are now 39 mm apart instead of the intended 40 mm as shown in Figure 8.4. This deformation of the main body does not impair the functionality of the MINT. No other deformations were observed in this test.

Little literature on repetitive sterilization of SLS PA-12 exist. One article evaluated the mechanical properties of this material and detected a decrease down to 77% of residual strength after 75 sterilization cycles [26]. As further research on the topic has not been found, it is not advisable to use the MINT over 75 times without investigating the degradation of the mechanical properties of SLS PA-12 for larger amounts of reprocessing cycles.

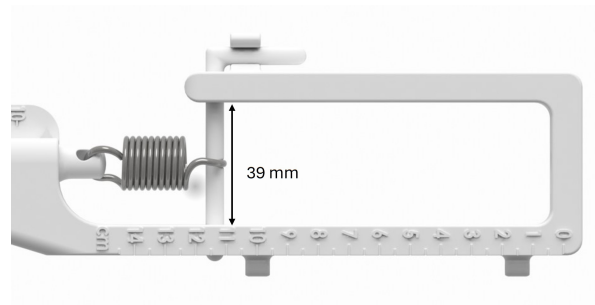


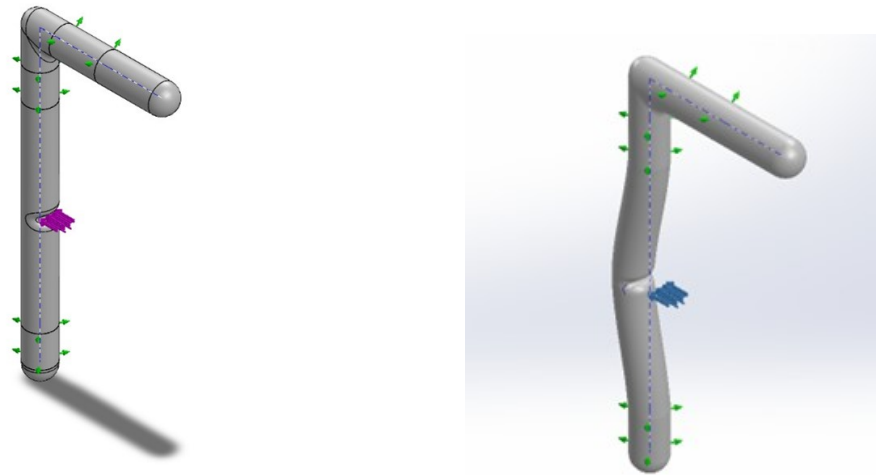
Figure 8.4: Front part of the MINT showing the deformation after ten sterilization cycles. The indicated width was 40 mm before sterilization.

8.4. Finite element analysis

The device has to be safe to use and should be able to withstand a maximum pulling force of 50 N. To assess this, a finite element analysis (FEA) was performed on the L-shaped link (red in Figure 6.2b) which is considered to be the component most likely to fail as it is the smallest component. In this analysis, the main body was replaced with fixtures and an external force of 50 N was applied in the notch for the spring (see Figure 8.5a). In some cases where material properties were provided as a range, such as the Yield stress ranging from 40 to 45 MPa [26]. For these properties, the most conservative value was always chosen to ensure a safer design, i.e., the value that would result in the highest stress and, consequently, the most stringent test conditions.

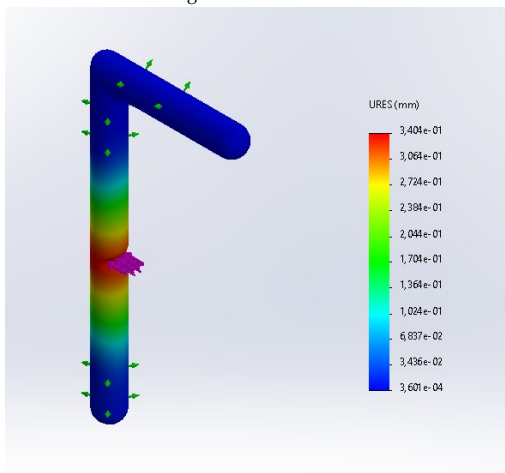
The analysis found a maximum displacement of 0.34 mm. This deformation is visualized in Figure 8.5b which scaled the displacement by 10. Figure 8.5c contains a non deformed displacement plot. The recorded displacement of 0.34 mm does not impair functionality of the MINT.

In this study also the Von Mises stress was calculated. It was found that the maximum stress is found in the notch for the spring and has a magnitude of 29.14 MPa. The yield stress of SLS PA-12 is 40-45 MPa and thus no plastic deformation (and breakage) is to be expected [26]. The yield stress of SLS PA-12 degrades under influence of sterilization cycles. After 75 sterilization cycles, a decrease in yield stress to 77% thus 30.8-34.65 MPa could be expected [26]. As these values lie close to the maximum Von Mises stress, it could be advisable to increase the radius of the L-shaped link.

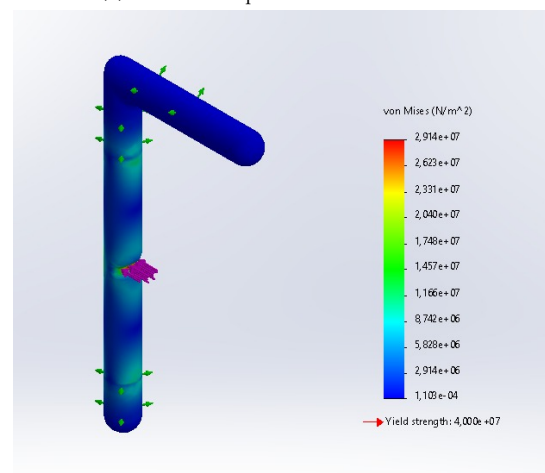


(a) Loading conditions: purple arrows indicating the 50 N external force, and the green arrows the fixtures.

(b) Deformed shape. Deformation scale: 10.



(c) Deformation of the L-shaped link.



(d) Von Mises stress in the L-shaped link.

Figure 8.5: FEA plots of the L-shaped link under assumption of the maximum applied force of the MINT (50 N).

8.5. Verification summary

This section provides a summary of the verification tests. In Table 8.2, the requirements from Table 4.1 are repeated with color coding to indicate the results: green for met requirements, orange for requirements that require additional clinical validation and red for unmet requirements. Subsections 8.5.1 and 8.5.2 entail explanation on the two requirements that have not been met (regarding the 1000 sterilization cycles and the width respectively). Subsection 8.5.3 provides explanation on the three orange requirements which require additional clinical validation.

Table 8.2: The requirements from Table 4.1 color coded based on the verification.

Green: the requirement has been met. Orange: the requirement requires additional clinical validation. Red: the requirement has not been met.

The device must	The device should	The device should not	The device must not
Be safe to use (both for the OR-staff and the patient).	Have less than eight components.	Have small components which could fall through the gauze of the sterilization basket.	Damage or compromise the laparoscopic forceps.
Be able to measure the force required to medialize the hernia (maximum 50 N with an accuracy of ± 3 N).	Have an assembly time faster than two minutes.	Extend more than 20 cm behind the laparoscopic forceps.	Contain parts that should or could be introduced into the trocar or the body.
Be able to withstand 1000 sterilization cycles.	Have a clear readability.	Exceed 6 cm in width.	
Be able to measure the distance (maximum 10 cm with an accuracy of ± 2 mm).	Be compatible with a diversity of laparoscopic forceps.		
Be attachable to a laparoscopic forceps whilst withstanding a pulling force of 50 N.	Allow for calibration each year.		
Be able to be assembled by OR-staff wearing sterile gloves.	Allow the measurements to be taken within 5 minutes.		
Be operable by a single surgeon.	Weight less than 1 kg.		
Be operable by surgeons with hand sizes above size 6.	Be able to apply for a CE mark as a Class I medical device.		

8.5.1. Sterilization

The requirement "the device must be able to withstand 1000 sterilization cycles" has not been met by the design. As there is limited literature on steam sterilizing SLS PA-12 past 75 cycles, it cannot be precluded that the device will be able to withstand more than 75 cycles. Future research on the sterilization of SLS PA-12 is recommended to assess material properties past 75 cycles. However, it is unlikely that 1000 sterilization cycles can be achieved. Additionally, the radius of the L-shaped link should be increased to maintain safety with degraded material properties.

This verification study assumed that the device is suitable for cleaning and disinfection as no problems were foreseen by the DSMH of the RDGG. It is recommended to further test for cleanability and disinfection to assure safety.

8.5.2. Width

The requirement "the device should not exceed 6 cm in width" has not been met. The device measures 80 mm at its widest point. The width of the main body, without the protrusions, is 60 mm as can be seen in Figure 8.6. This width is required to allow for insertion of a commonly used laparoscopic forceps that has a turning knob with a width of 4 cm.

To reduce the width, alterations to the device could be considered: The first option to decrease the width would be placing the protrusions of the distance indicator on top of the main body instead of on the sides. The scale numbers that are now on top of the device could be placed on the side. This reduces the width with 6 mm. However, as the scale would then be at the side of the main body, taking measurements would require the surgeon to bend forward and twisting their head. This position is not only not ergonomic, but it could also introduce errors as maintaining the same tension on the fascia in this position is nearly impossible.

Another option could be placing the distance indicator inside the main body. This would reduce the width with 7 mm. However, this alteration introduces a narrow long hole in the design which could complicate the cleaning process.

Originally, this requirement was added based on expert input who suggested that a width above 6 cm would feel "bulky". Through surgeon feedback it was found that the device did not feel bulky, and that

the additional width added a feeling of robustness. Therefore, it was chosen to not implement any of the suggested alterations to the design.

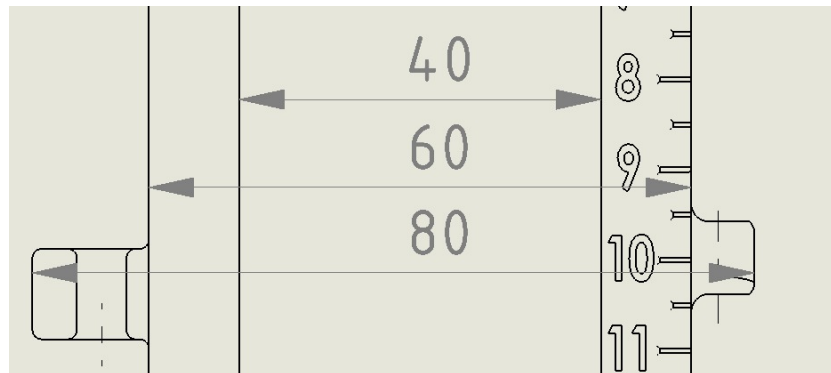


Figure 8.6: Width of the final design in mm.

8.5.3. Clinical validation

Three requirements have not been assessed in this verification study due to limitations of creating a representative, clinical, test setting (orange in Table 8.2). Clinical testing is advised for these requirements.

Distance measurement

The first requirement which requires further clinical testing is "the device must be able to measure the distance (maximum 10 cm with an accuracy of ± 2 mm)". To accurately test this requirement, a flexible abdominal wall is required. It is expected that an error in the distance measurement will occur. However, as it is expected that all cases will have roughly the same error, it is expected that this error will not influence the recommended procedure.

Measurement time

Obtaining measurements should be possible within five minutes according to the list of requirements. This requirement has not been tested as the resources to create a representative, clinical, test setting were not available. However, it is expected that the required measurements can be taken within five minutes.

Damage laparoscopic forceps

The requirement "the MINT must not damage or compromise the laparoscopic forceps" has not been tested. The edges on which the MINT and the laparoscopic forceps are in touch with each other, have been rounded to minimize the chance of damage. It is not expected that the laparoscopic forceps is compromised or subjected to damage. In case future testing indicates a possibility of compromising or damaging the laparoscopic forceps, a liner could be implemented between the MINT and the laparoscopic forceps.

9

Discussion

The outcome of this design study is an improved version of the MINT which can assess fascial tension to aid in surgical decision making. By focusing on redesigning the connection mechanism between the laparoscopic handle and the MINT, the component count has reduced significantly, exceeding expectations and the requirement of eight components. In this redesign, the shaft is used as the connection point for the MINT. As the shaft has the same width for all used laparoscopic graspers, the MINT can be mounted to a wide range of used models and brands of laparoscopic graspers and is only limited by the width of the handle as it is not compatible with handle widths over 4 cm. In addition, this connection has proven to be more reliable as assembly errors are not apparent in the new MINT, minimizing chance on disconnection and thus minimizing the chance of dangerous situations.

Furthermore, the five remaining components are larger in size which removes the chance of components falling through the sterilization basket and which makes the components easier to handle. Additionally, no tools are required for the assembly or disassembly of the device. These improvements make the MINT more suitable for reprocessing and easier to assemble, which makes the device more suitable for implementation during herniorrhaphies.

In this chapter the limitations of this research will be defined and recommendations will be given for the future steps of the MINT.

9.1. Limitations

Some limitations should be noted about this study. Firstly, it should be noted that in this study a verification study of the device was performed, intended to check if the device meets the set of design requirements. No validation study was performed and thus it cannot be precluded that the device meets the operational needs of the user. A validation study must be performed before the implementation of the device. Additionally, three requirements require future clinical testing as they have not yet been evaluated due to limited resources.

Secondly, this study was performed to make a device that could be implemented as easily as possible. Therefore, it was chosen to have Oceanz as a manufacturer as they commonly deliver 3D printed parts to the TU Delft and they are ISO 13485 certified with which they can also provide a medical declaration of conformity for their SLS PA-12 parts. Some other materials have been considered but no elaborate material study was performed. Therefore, it cannot be precluded that this material is the most suitable material for the application.

Thirdly, the device was not loaded until failure as it is expected that this load will not be applied to the MINT within regular use. Therefore, it was left out of the thesis. However, it may be useful to explore this in the future.

Next, in the study ten sterilization cycles were completed to test for possible deformations. Resources to assess changes in mechanical properties, such as yield strength, were not available and thus not recorded. Additionally, only ten sterilization cycles were completed due to time limitations. Completing more

sterilization cycles in future research could provide additional insights into the change of mechanical properties and the deformation of the SLS PA-12 parts.

Next, as mentioned in Section 6.2.1, the specifications of the spring differed from the specifications provided by the manufacturer. The reason behind this difference was seen as outside of the scope of this research. Explanations of these differences could be plastic deformation or manufacturing errors. These two factors would not impair the functionality of the device if calibration tests are implemented before the first use of the device. Another theory could be that sterilization cycles could act as a type of heat treatment which could influence the mechanical properties over time (IWS, personal communication, May 2, 2024). This would influence the accuracy of the device over time. In case this theory appears to be true, it is recommended to change the spring material, to increase the frequency of calibration or to frequently replace the spring for a new spring.

Another limitation within the design of the force measurement system was found in the verification device. The electronic scale used in this verification step said to have an accuracy of 10 grams (roughly 0.1 N). However, during the verification test suspicion on this accuracy arose as the device indicated a larger difference with the same applied force. It is recommended to repeat this test with a different, more reliable, calibration device. The offset in this test could be explained by inaccuracy of the weights used in the tests which had mass indications on the weights but seemed dented.

Next, as the main goal of this study is to minimize the number of components, compliant mechanisms have been considered. Benefits of such mechanisms are that they are monolithic (existing from one part) and thus do not require assembly. Several embodiments of compliant mechanisms have been evaluated but all showed the same limitations. These limitations include their manufacturability and the small deflection and thus a small measuring scale. These problems could be solved by scaling the design. However, this would make the design rather large. Therefore, this thesis only focused on a design including a traditional tension spring.

Finally, the device is made for use in minimally invasive ventral abdominal wall hernia repair. In these surgeries insufflation of the abdominal cavity is used to generate a suitable workspace for the surgeon. As this pneumoperitoneum creates an internal pressure on the abdominal wall, it is likely that the force and distance measurements are dependent on the pressure. This influence has not been quantified in this study. Using the same pressure for all patients could minimize the influence of the pneumoperitoneum on the obtained measurements. For this a pressure of 8 mm Hg is advised. If this pressure cannot be used on a patient, the measurement should not be integrated in the data set of the other measurements.

9.2. Recommendations

The goal of this project was to design a device which could be safely and effectively implemented in herniorrhaphies across Europe to provide surgeons with intraoperative quantitative data to aid in decision making. The design presented in this thesis has been significantly simplified in comparison to the MINT designed by E.F. van Koten and is thus more suitable for implementation in the OR. To do this safely, the following future steps should be considered.

In this thesis, a verification study was performed based on the set of requirements. During this verification study, not all requirements have been evaluated. It is advised to complete the verification study by computing clinical tests on the three not yet evaluated requirements (the distance measurement, measurement time, and damage/compromising the laparoscopic forceps). Additionally, additional testing on reprocessing should be done to estimate the number of reuses of the device. Increasing the radius of the L-shaped link is advised if the device were to complete 75 reprocessing cycles.

In this verification study, the device was assumed to be safe as the device contains no sharp edges and no components can come loose during operation of the device. Furthermore, the chance of assembly errors has been reduced and thus the chance of unsafe situations due to those errors is lower compared to the original MINT. This was endorsed by surgeon feedback which stated that the MINT is "foolproof". It is recommended to complete a Failure Modes and Effects Analysis (FMEA) to identify and assess all risks.

After these tests, it could be useful to further investigate the design by completing a validation study. In this study, more realistic settings (such as cadaver tests) could be used.

The MINT can provide surgeons intraoperative data regarding quantified fascial tension. This measurement technique should be further refined by addressing the number and location of attachment points of the laparoscopic forceps to the fascia. Additionally, no interpretation of these data yet exists. Therefore, a large-scale study should be aimed at finding correlations between these data and long-term patient outcomes. These correlations combined with patient specifics can then aid in decision making for future patients.

10

Conclusion

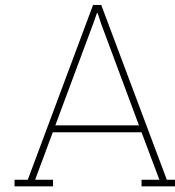
This research aimed to design a device for use in laparoscopic herniorrhaphy to provide intraoperative information on fascial tension to the surgeon in aim of reducing recurrence rates. For this, the MINT designed by E.F. van Koten is used as starting point. The main challenge of this design was the complexity and the number of components. By redirecting the clamping mechanism from a friction-based clamp towards a clamping mechanism based on a male-female connection, the component count was reduced significantly to five components. This reduction eases the assembly, disassembly, cleaning, and sterilization process, making the design more suitable for implementation. Functionality is substantiated through several technical tests focused on verification of the design requirements. Although results are promising, further research is needed to prove functionality and safety in clinical settings. Results indicate that the new design can withstand at least ten steam sterilization cycles. Further studies must be conducted to assess the mechanical degradation and reprocessing compatibility of SLS PA-12 for reusable medical devices. Implementation of the improved MINT can help surgeons objectively assess fascial tension and could provide data necessary to decrease the 30% recurrence rate and to improve patient care.

References

- [1] Jiting Yang et al. *Pore Texture Analysis in Automated 3D Breast Ultrasound Images for Implanted Lightweight Hernia Mesh Identification: A Preliminary Study*. July 2020. DOI: 10.21203/rs.3.rs-50242/v1.
- [2] Raquel Maia et al. "Ventral hernia and obesity: is there a consensus?" en. In: *Annals of Laparoscopic and Endoscopic Surgery* 4.0 (Feb. 2019). Number: 0 Publisher: AME Publishing Company. ISSN: 2518-6973. DOI: 10.21037/ales.2019.01.07. URL: <https://ales.amegroups.org/article/view/5013> (visited on 06/22/2024).
- [3] Corey R. Deeken and Spencer P. Lake. "Mechanical properties of the abdominal wall and biomaterials utilized for hernia repair". In: *Journal of the Mechanical Behavior of Biomedical Materials* 74 (Oct. 2017), pp. 411–427. ISSN: 1751-6161. DOI: 10.1016/j.jmbbm.2017.05.008. URL: <https://www.sciencedirect.com/science/article/pii/S1751616117301960> (visited on 06/02/2024).
- [4] Upstate University Hospital. *About Hernias | Hernia Surgery*. en-US. URL: <https://www.upstate.edu/hernia/about-hernia/index.php> (visited on 05/28/2024).
- [5] Paul L. Tenzel et al. "Tension measurements in abdominal wall hernia repair: Concept and clinical applications". en-US. In: *International Journal of Abdominal Wall and Hernia Surgery* 2.4 (Dec. 2019), p. 119. ISSN: 2589-8736. DOI: 10.4103/ijawhs.ijawhs_37_19. URL: https://journals-lww-com.tudelft.idm.oclc.org/rhaw/fulltext/2019/02040/tension_measurements_in_abdominal_wall_hernia.1.aspx (visited on 06/04/2024).
- [6] N. N. Baastrup et al. "Visceral obesity is a predictor of surgical site occurrence and hernia recurrence after open abdominal wall reconstruction". en. In: *Hernia* 26.1 (Feb. 2022), pp. 149–155. ISSN: 1248-9204. DOI: 10.1007/s10029-021-02522-5. URL: <https://doi.org/10.1007/s10029-021-02522-5> (visited on 06/22/2024).
- [7] Julia Hamilton et al. "Age-Related Risk Factors in Ventral Hernia Repairs: A Review and Call to Action". In: *Journal of Surgical Research* 266 (Oct. 2021), pp. 180–191. ISSN: 0022-4804. DOI: 10.1016/j.jss.2021.04.004. URL: <https://www.sciencedirect.com/science/article/pii/S0022480421002328> (visited on 06/22/2024).
- [8] A. S. Levy et al. "Quantifying fascial tension in ventral hernia repair and component separation". en. In: *Hernia* 25.1 (Feb. 2021), pp. 107–114. ISSN: 1248-9204. DOI: 10.1007/s10029-020-02268-6. URL: <https://doi.org/10.1007/s10029-020-02268-6> (visited on 06/22/2024).
- [9] Yewande Alimi et al. "Mesh and plane selection: a summary of options and outcomes". en. In: *Plastic and Aesthetic Research* 7.0 (Feb. 2020). Publisher: OAE Publishing Inc., N/A–N/A. ISSN: ISSN 2349-6150 (Online)
ISSN 2347-9264 (Print). DOI: 10.20517/2347-9264.2019.39. URL: <https://www.oaepublish.com/articles/2347-9264.2019.39> (visited on 06/02/2024).
- [10] William W. Hope et al. "Rationale and Technique for Measuring Abdominal Wall Tension in Hernia Repair". eng. In: *The American Surgeon* 84.9 (Sept. 2018), pp. 1446–1449. ISSN: 1555-9823.
- [11] Eveline Van Koten. "MINT: Minimally INvasive Tensiometry: A novel method to assess laparoscopic herniorrhaphy". en. In: (2021). URL: <https://repository.tudelft.nl/islandora/object/uuid%3Aeb17263b-bbec-4e01-8841-e1749e704ea6> (visited on 01/18/2024).
- [12] Benjamin T. Miller et al. "Physiologic tension of the abdominal wall". en. In: *Surgical Endoscopy* 37.12 (Dec. 2023), pp. 9347–9350. ISSN: 1432-2218. DOI: 10.1007/s00464-023-10346-w. URL: <https://doi.org/10.1007/s00464-023-10346-w> (visited on 06/22/2024).
- [13] Leonard Frederik Kroese. *Closing gaps - risk factors, occurrence, and treatment of abdominal wall hernias*. PhD thesis. 2018, ISBN: 9789463750042.

- [14] Hamid Reza Zahiri, Igor Belyansky, and Adrian Park. "Abdominal Wall Hernia". In: *Current Problems in Surgery* 55.8 (Aug. 2018), pp. 286–317. ISSN: 0011-3840. DOI: 10.1067/j.cpsurg.2018.08.005. URL: <https://www.sciencedirect.com/science/article/pii/S0011384018301254> (visited on 05/30/2024).
- [15] William Flynn and Paula Vickerton. "Anatomy, Abdomen and Pelvis: Abdominal Wall". eng. In: *StatPearls*. Treasure Island (FL): StatPearls Publishing, 2024. URL: <http://www.ncbi.nlm.nih.gov/books/NBK551649/> (visited on 05/28/2024).
- [16] Milind Kachare et al. "Incisional Hernia After Percutaneous Endoscopic Gastrostomy Tube Placement: Importance of Avoiding the Linea Alba". In: *ACG Case Reports Journal* 6 (July 2019), p. 1. DOI: 10.14309/crj.000000000000120.
- [17] Elaine Nicpon Marieb and Katja Hoehn. *Human Anatomy & Physiology*. en. 11th ed. Pearson Education, 2019. ISBN: 978-1-292-26085-3.
- [18] James J. Mensching and Anthony J. Musielewicz. "ABDOMINAL WALL HERNIAS* *". English. In: *Emergency Medicine Clinics* 14.4 (Nov. 1996). Publisher: Elsevier, pp. 739–756. ISSN: 0733-8627, 1558-0539. DOI: 10.1016/S0733-8627(05)70277-7. URL: [https://www.emed.theclinics.com/article/S0733-8627\(05\)70277-7/fulltext](https://www.emed.theclinics.com/article/S0733-8627(05)70277-7/fulltext) (visited on 05/28/2024).
- [19] Bingley. *PERFORATED INSTRUMENT TRAY*. zh-CN. Section: Side Show. Oct. 2010. URL: <http://www.fineartsmed.com/perforated-instrument-tray/> (visited on 05/29/2024).
- [20] Marloes Femke Wempe. *Gripping mechanisms: A systematic patent review for the improvement of abdominal wall tension measurements during minimally invasive herniorrhaphy*. Unpublished manuscript, Contact: author for access. 2024.
- [21] *Teveva T42010*. URL: <https://webshop.tevema.com/nl/t42010> (visited on 05/18/2024).
- [22] *Oceanz 3D printing Ede - Professioneel 3D printen*. nl-NL. URL: <https://www.oceanz.eu/> (visited on 03/26/2024).
- [23] Davood Rouholamin and Neil Hopkinson. "An investigation on the suitability of micro-computed tomography as a non-destructive technique to assess the morphology of laser sintered nylon 12 parts". en. In: *Proceedings of the Institution of Mechanical Engineers, Part B: Journal of Engineering Manufacture* 228.12 (Dec. 2014). Publisher: IMECHE, pp. 1529–1542. ISSN: 0954-4054. DOI: 10.1177/0954405414522209. URL: <https://doi.org/10.1177/0954405414522209> (visited on 06/06/2024).
- [24] J.P. Kruth et al. "Lasers and materials in selective laser sintering". In: *Assembly Automation* 23.4 (Jan. 2003). Publisher: MCB UP Ltd, pp. 357–371. ISSN: 0144-5154. DOI: 10.1108/01445150310698652. URL: <https://doi.org/10.1108/01445150310698652> (visited on 06/26/2024).
- [25] *RVS rondstaf AiSi 316 blank getrokken H9*. nl. URL: <https://www.metaalwinkelonline.nl/rvs-rondstaf-316.html> (visited on 05/31/2024).
- [26] Miriam Haerst et al. "Ageing processes in laser sintered and injection moulded PA12 following hygienic reprocessing". In: *Rapid Prototyping Journal* 21 (Apr. 2015), pp. 279–286. DOI: 10.1108/RPJ-06-2013-0061.

Appendices



Spring Calibration

In this appendix the acquired data during the spring calibration tests are listed in Table A.1. With this data an estimation of the force deflection curve was made (Figure A.1).

Table A.1: Data of the spring calibration.

Mass (kg)	Force (N)	Length (mm)	Deflection (mm)
0	0	43.3	-
0.75	7.3575	50.0	6.7
1.18	11.5758	53.9	10.6
1.25	12.2628	55.8	12.5
1.85	18.1485	61.0	17.7
2.00	19.62	65.5	22.2
3.10	30.411	75.8	32.5
3.85	37.7685	87.0	43.7
4.28	41.9868	90.0	46.7
5.03	49.3443	99.5	56.2

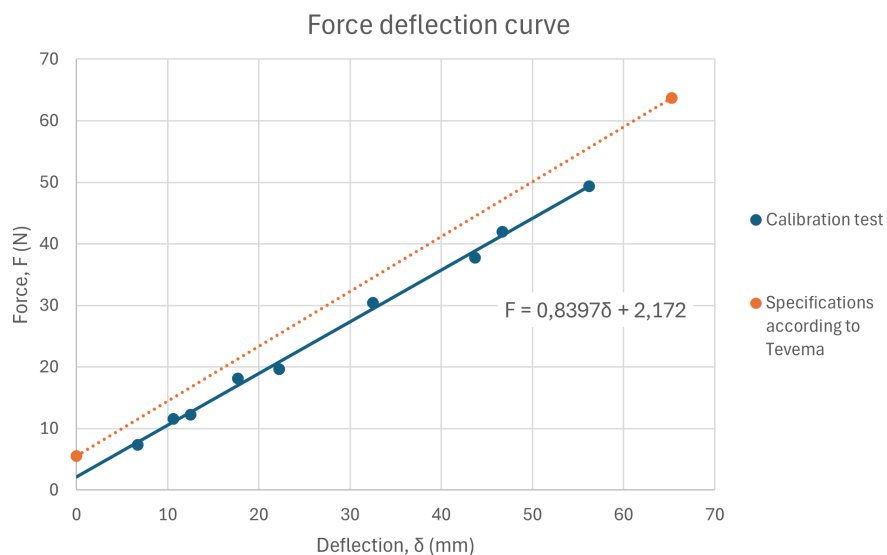


Figure A.1: The force deflection curve of the spring based on the data in Table A.1. The trend line is based on the least square error method. The other force deflection curve is based on the manufacturer specifications.

B

Harris Profile Scores

In this appendix a table containing the reasoning of the scores in Subsection 6.3.2 is provided (Table B.1).

Table B.1: Reasoning behind the Harris profile in Subsection 6.2.

	1	2	3	4	5	6
Ease of use	An additional operator is necessary for the placement of the finger during the whole procedure.	The device can be operated by one operator.	The device can be operated by one operator.	An additional operator is necessary during the distance measurement.	The device can be operated by one operator.	The device can be operated by one operator.
Intuitiveness	Intuitive	Intuitive	Intuitive	Intuitive	Intuitive	Not intuitive
Number of components	1	2	1	2	1	1
Measurement error	The finger is prone to movements and could introduce a measurement error.	No measurement errors are expected.	No measurement errors are expected.	No measurement errors are expected.	No measurement errors are expected.	A minor measurement error can be expected as there most likely is an offset between the remembered indicator and 0.
Mathematics	No mathematical steps required	No mathematical steps required	Subtraction of two values	No mathematical steps required	Subtraction of two values	No mathematical steps required
Width	Width of a ruler + a small holder	Width of a ruler + movable holder	Width of a ruler + small holder	Width of a thin rod + small holder	Width of a thin rod + small holder	Width of a ruler + small holder

C

General Dimensions MINT

This Appendix provides the technical drawings showing the most important dimensions of the main body, the L-shaped link, the handle, and the distance indicator (Figures C.1, C.2, C.3 and C.4).

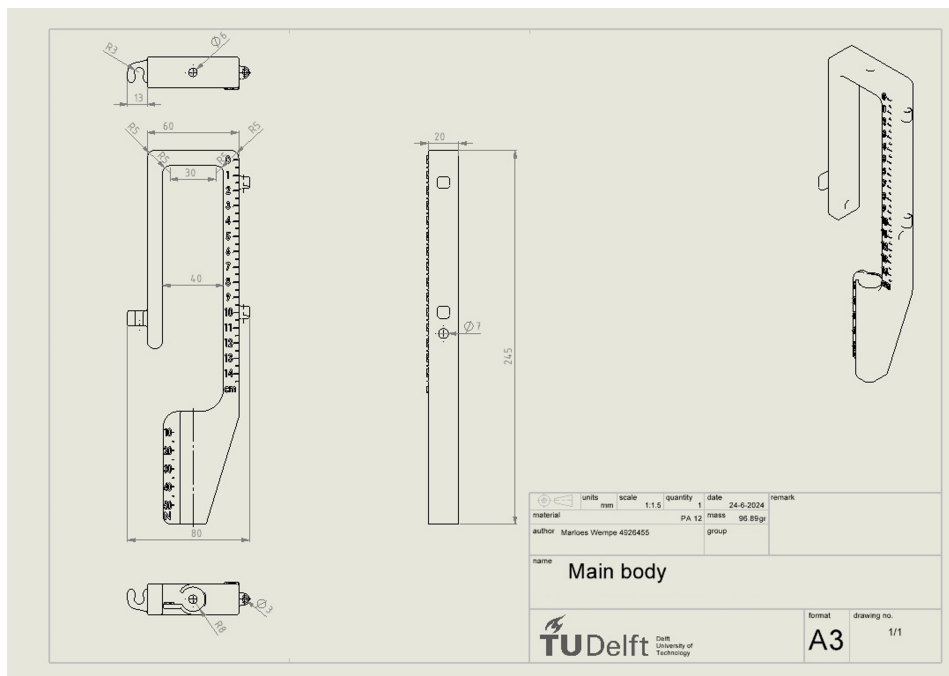


Figure C.1: Technical drawing of the main body.

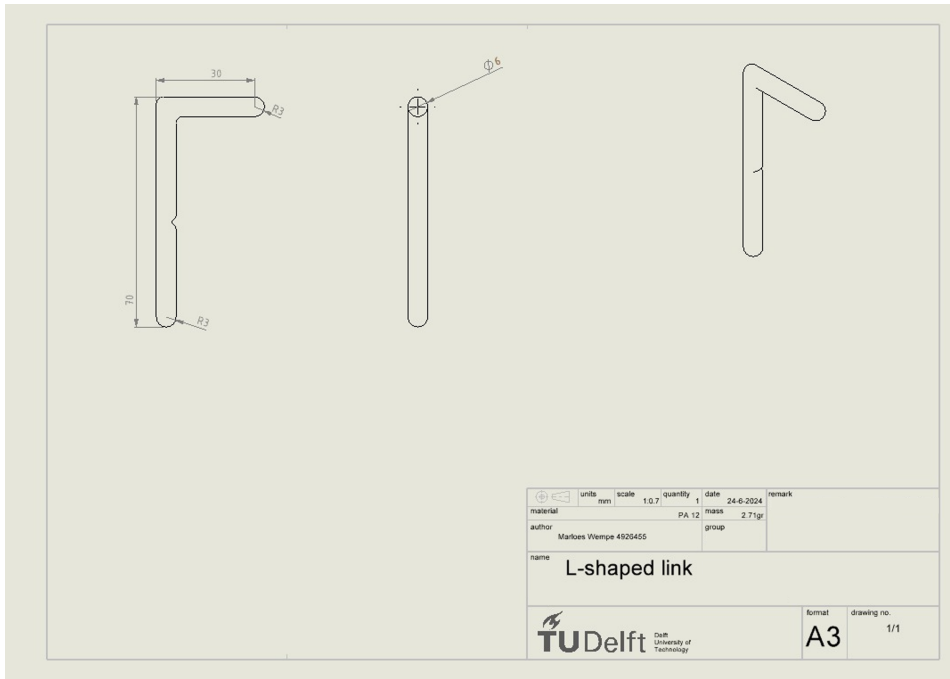


Figure C.2: Technical drawing of the L-shaped link.

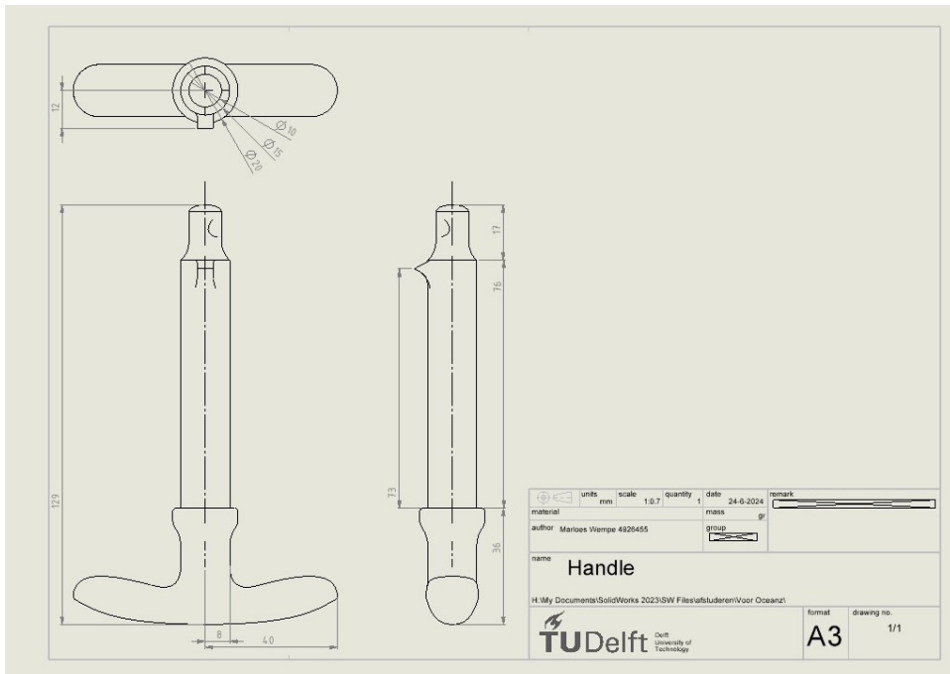


Figure C.3: Technical drawing of the handle.

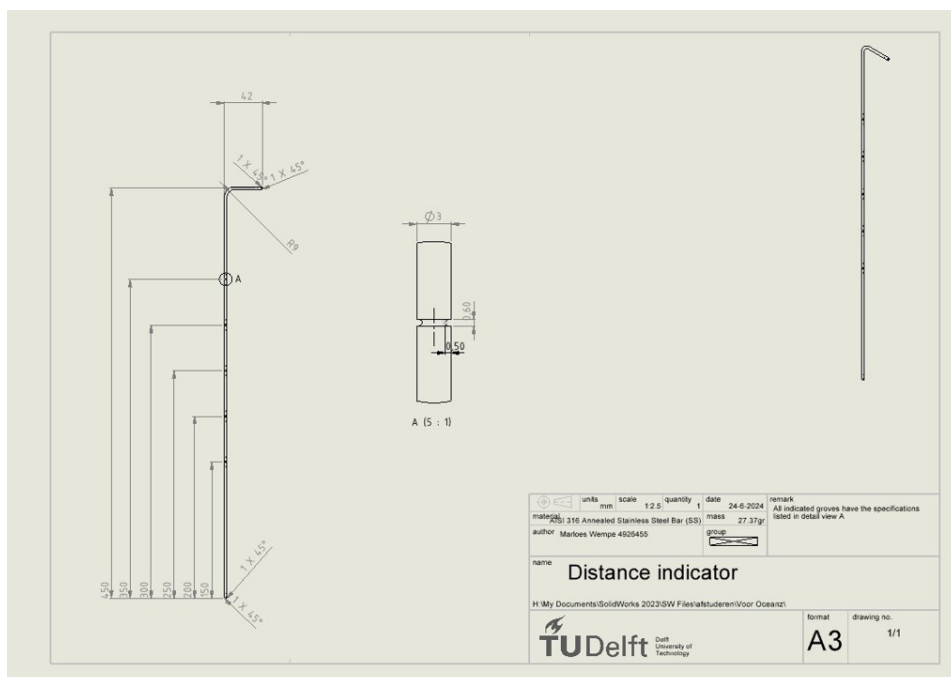


Figure C.4: Technical drawing of the distance indicator.

D

Instruction Manual

This appendix contains the instruction manual. This manual contains information on the components, on the assembly, use and disassembly of the MINT. Furthermore, the last page contains the instructions for printing the SLS PA-12 components.

MINIMALLY INVASIVE
TENSIOOMETRY

MINT

INSTRUCTION MANUAL



 **TU Delft**

Reinier de Graaf 

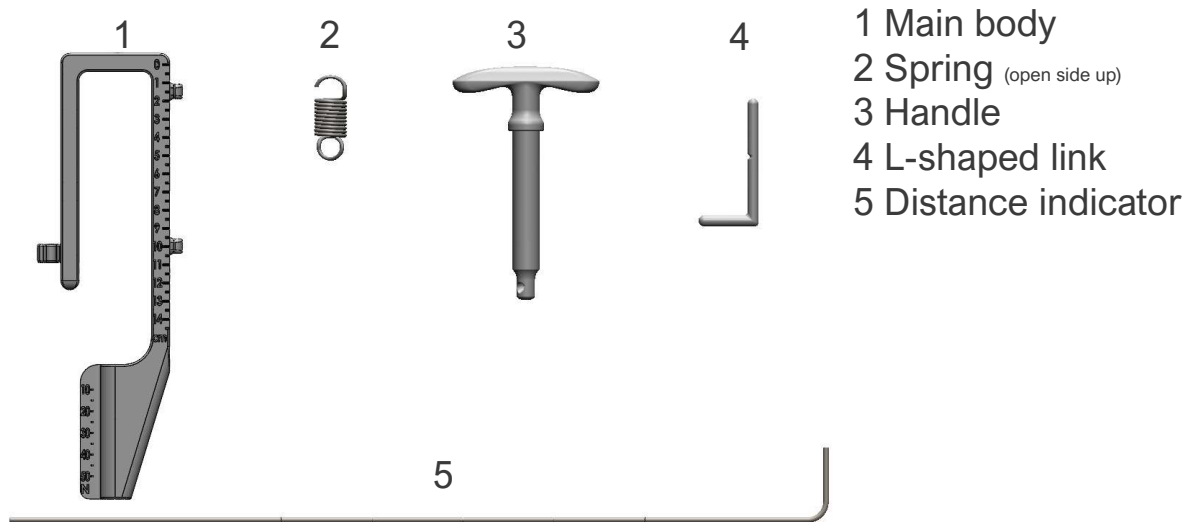
MINT – MINIMALLY INVASIVE TENSIOOMETRY INSTRUCTION MANUAL

In this manual, instructions will be given for the assembly and use of MINT. The device can be disassembled by performing steps 1 through 6 in reverse order.

The measurements obtained by the device should be obtained at an insufflation pressure of 8mm Hg.

WARNING: If this pressure leads to unsafe conditions, do **NOT** use this pressure. Instead, use a pressure appropriate for the patient and make sure the different pressure is recorded.

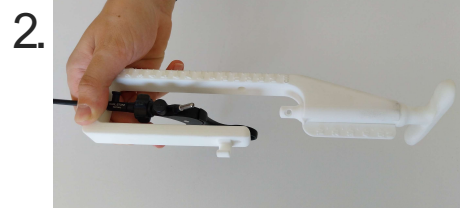
MINT – MINIMALLY INVASIVE TENSIOMETRY INSTRUCTION MANUAL



MINT – MINIMALLY INVASIVE TENSIOMETRY INSTRUCTION MANUAL



Insert the laparoscopic shaft through the front cavity of the main body.



Slide the handle into the main body.



Insert the open side of the spring through the opening in the handle.



Slide the L-shaped link through both holes in the main body, passing through the closed side of the spring.

MINT – MINIMALLY INVASIVE TENSIOMETRY INSTRUCTION MANUAL

5.



Rotate the L-shaped link counterclockwise to secure it in place.

6.



Insert the distance indicator through the holes at the right side of the main body.

MINT – MINIMALLY INVASIVE TENSIOMETRY INSTRUCTION MANUAL

Use

1. Check if the insufflation pressure is at 8 mm Hg and grab the to be measured tissue with the laparoscopic grasper.
2. Place the distance indicator against the skin/trocar.
3. Read the value indicated by the distance indicator.
4. Pull on the handle till the tissue reaches the required medialization. Do NOT touch the laparoscopic forceps. **WARNING: Do not apply more force to the tissue than you would normally apply (without the MINT) to avoid causing tissue damage.**
5. Read the value of the force indicated by the arrow on the handle. Do NOT touch the laparoscopic forceps.
6. Push the tip of the distance indicator against the skin/trocar.
7. Read the value indicated by the distance indicator.
8. Release the tension and then let go of the tissue.

The medialized distance can be obtained by subtracting the measurement in step 6 from the measurement in step 2.

The force measurement is obtained in step 4.

MINT – MINIMALLY INVASIVE TENSIOMETRY INSTRUCTION MANUAL

INSTRUCTIONS FOR PRINTING

All printed parts are selective laser sintered in PA-12 conform to ISO 13485 by OCEANZ. The following settings should be applied:

Application Medical	Sterile Yes
Intended use No direct contact with patient	Clinical use Yes
Material Oceanz PA12	Colour No colouring
Polishing No	Orientation unlocked



MINIMALLY INVASIVE
TENSIOMETRY

MINT

INSTRUCTION MANUAL

 **TU Delft**

Reinier de Graaf 

E

Verification Data

In this appendix the acquired data during the force measurements and the assembly/disassembly measurements are provided.

E.1. Force measurement test

This section contains the data obtained in the test mentioned in Section 8.1. To assess the accuracy of the device an electronic scale was placed in line with the MINT. Tension was applied to the device and the corresponding measured value on the electronic scale was documented (in kg). Each measurement was repeated four times, after which the force was increased with 5 N. Results can be seen in Table E.1. The force gauge (in N) was computed by multiplying the mass indicated by the electronic scale by the gravitational acceleration (9.81 m/s^2).

Table E.1: Force gauge verification data.

Force MINT (N)	Portable electronic scale (kg)	Force Gauge (N)	Error (N)
10	1.11	10.8891	0.8891
10	1.11	10.8891	0.8891
10	1.06	10.3986	0.3986
10	1.06	10.3986	0.3986
15	1.595	15.64695	0.64695
15	1.62	15.8922	0.8922
15	1.61	15.7941	0.7941
15	1.575	15.45075	0.45075
20	2.16	21.1896	1.1896
20	2.17	21.2877	1.2877
20	2.18	21.3858	1.3858
20	2.15	21.0915	1.0915
25	2.71	26.5851	1.5851
25	2.69	26.3889	1.3889
25	2.66	26.0946	1.0946
25	2.69	26.3889	1.3889
30	3.23	31.6863	1.6863
30	3.18	31.1958	1.1958
30	3.25	31.8825	1.8825
30	3.26	31.9806	1.9806
35	3.735	36.64035	1.64035
35	3.79	37.1799	2.1799
35	3.81	37.3761	2.3761
35	3.64	35.7084	0.7084
40	4.29	42.0849	2.0849
40	4.27	41.8887	1.8887
40	4.155	40.76055	0.76055
40	4.34	42.5754	2.5754
45	4.875	47.82375	2.82375
45	4.85	47.5785	2.5785
45	4.77	46.7937	1.7937
45	4.69	46.0089	1.0089
50	5.30	51.993	1.993
50	5.39	52.8759	2.8759
50	5.255	51.55155	1.55155
50	5.34	52.3854	2.3854
		Mean Error	1.492825 N

E.2. Assembly and disassembly test

This section provides the data of the assembly and disassembly tests as discussed in Section 8.2 in Table E.2.

Table E.2: Assembly and disassembly data (minutes : seconds) of the MINT designed by E.F. van Koten and the new design.

	MINT of E.F. van Koten		New MINT		
	Assembly	Disassembly	Assembly	Disassembly	
Novice	1	05:09	01:39	00:37	00:11
	2	03:06	01:07	00:20	00:10
	3	03:04	01:07	00:18	00:09
	4	02:04	01:15	00:26	00:09
	5	02:07	01:11	00:17	00:08
	6	-	01:01	00:20	00:08
	7	02:10	00:55	00:18	00:08
	8	01:57	00:56	00:19	00:10
	9	01:46	00:52	00:19	00:08
	10	01:40	00:54	00:21	00:09
Mean	02:33	01:05	00:21	00:09	
Advanced	1	02:30	01:14	00:36	00:08
	2	02:19	01:04	00:25	00:09
	3	01:57	01:01	00:22	00:14
	4	02:03	00:57	00:24	00:08
	5	02:02	00:51	00:38	00:08
	6	02:00	00:56	00:27	00:10
	7	02:05	00:50	00:19	00:07
	8	01:45	01:10	00:17	00:08
	9	-	01:18	00:18	00:07
	10	02:13	00:57	00:21	00:09
Mean	02:06	01:01	00:24	00:08	

On this data-set several remarks have to be made:

- In this table no times were registered for the assembly test number six of the novice participant and test nine for the advanced participant. In these two tests, a component fell on the "not sterile" floor during the assembly. It was chosen to not include these assembly times as the complete assembly and use of the MINT would not be possible in the surgery.
- In the first assembly test of the novice participant, the MINT of E.F van Koten was incorrectly mounted onto the laparoscopic grasper. The participant did not notice the difference between the shorter side of the "moving block" and the other side (step 9 and 10 in the protocol of said design). Therefore, this component was placed the wrong way around and the connection between the MINT and laparoscopic grasper was not secure. In this test setting, the MINT became loose but no harm was done, however, in a surgical setting, it could be dangerous.
- In this test frustration levels were not measured. However, the participants expressed to be frustrated and feel stressed during the assembly and disassembly of the MINT designed by E.F. van Koten. They did not express this concern during the assembly and disassembly of the new MINT.